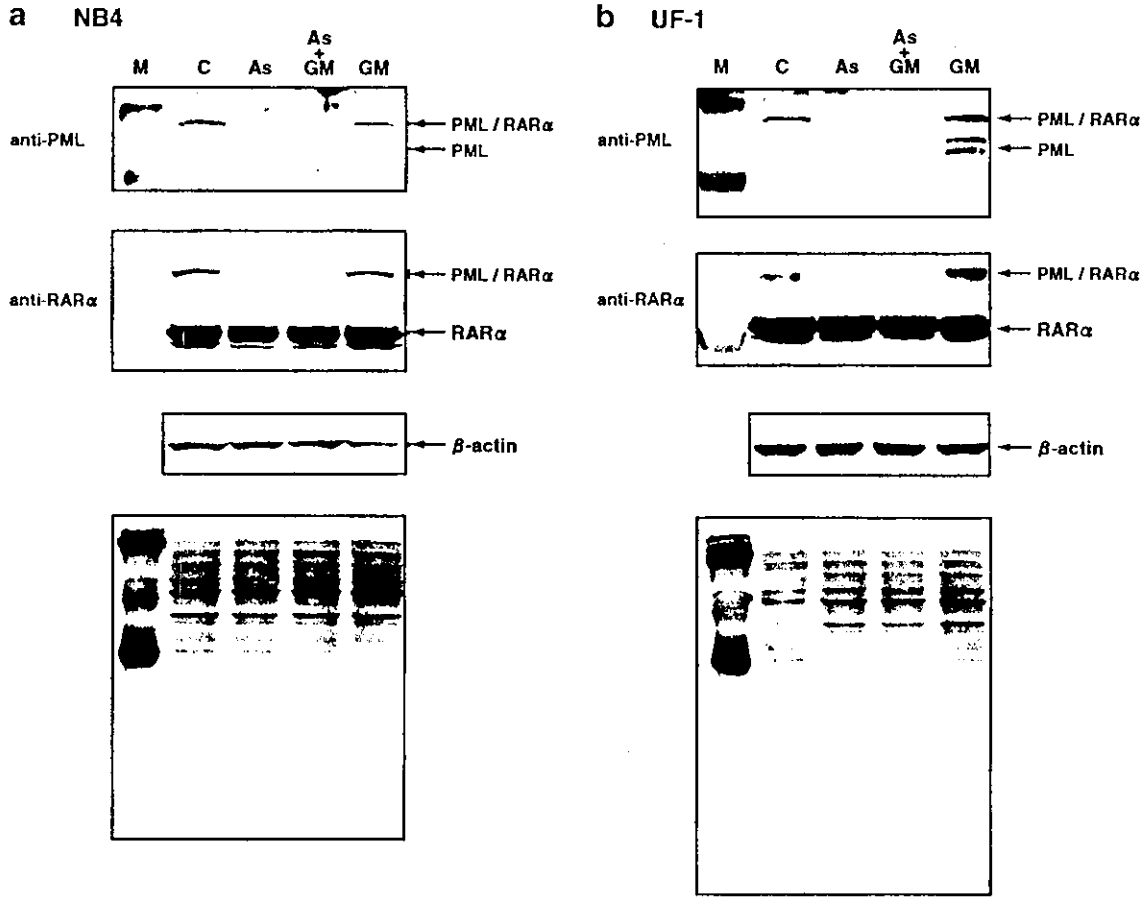

Figure 3 Western blot analysis of PML/RARα and RARα expression in APL cells. NB4 cells (a) and UF-1 cells (b) were cultured for 6 h with medium alone (C), with 1 μM As_2O_3 (As), with a combination of 10 ng/ml GM-CSF and 1 μM As_2O_3 (As + GM), or with 10 ng/ml GM-CSF (GM). Cell lysates (10 μg of protein per lane) were fractionated in 12.5% SDS-polyacrylamide gel and analyzed by Western blotting using an anti-PML (upper panel), anti-RARα (middle panel) and anti-β-actin (lower panel) antibodies. Blots were also stained with Coomasie brilliant blue to confirm that equal amounts of protein were present in each lane. M: molecular weight marker.

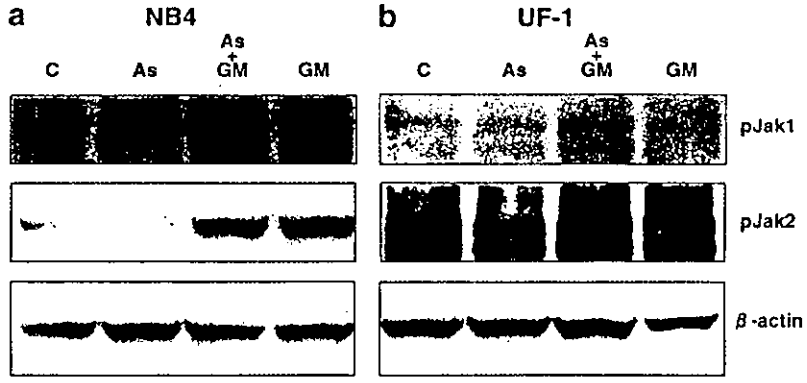

Figure 4 Jak2, but not Jak1, is activated by the treatment of GM-CSF with or without As_2O_3 in APL cells. NB4 cells (a) and UF-1 cells (b) were cultured with 1 μM As_2O_3, a combination of 10 ng/ml GM-CSF and 1 μM As_2O_3, or 10 ng/ml GM-CSF alone for 5 min. Cell lysates were analyzed by Western blotting using anti-Jak1 and -Jak2 dual phosphospecific antibodies. The figure shows phosphorylated Jak1 and Jak2 in UF-1 cells treated with the indicated chemicals.

in vivo by means of this hGMTgSCID mouse system. As previously reported,[25] As_2O_3 suppressed the growth of subcutaneous tumors to about half of the initial size in the APL mice, who showed high serum levels of human GM-CSF. After treatment with As_2O_3 for 21 days, mice were sacrificed and tumors were histologically examined. Interestingly, in contrast to PBS-treated control tumors, As_2O_3-treated tumors showed mature granulocytes and no observable leukemic cells (Figure 7a). These mature granulocytes were positive for anti-human MPO, LCA and neutrophil esterase antibodies (Figure 7b). These antibodies were specific for human tissues and did not cross-react with cells from mouse tissues. Therefore, these his-

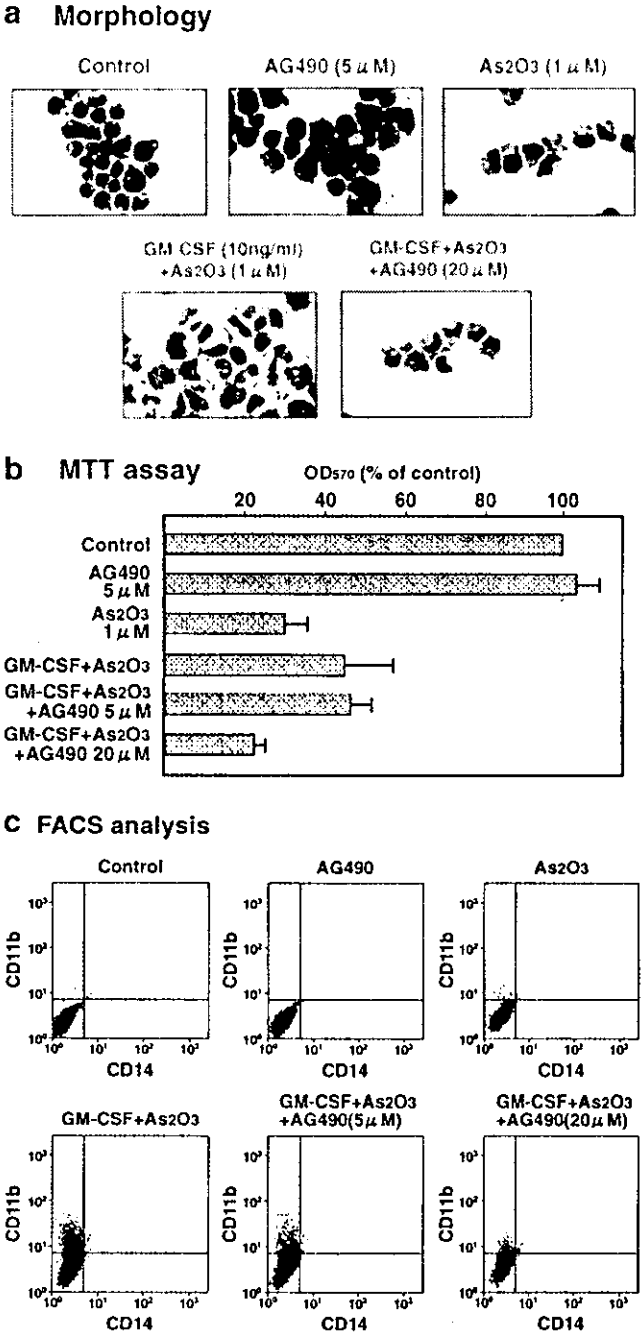

Figure 5 Effects of the Jak2 kinase inhibitor, AG490, on cell survival and differentiation of APL cells. UF-1 cells were cultured in the presence of the indicated chemicals for 4 days, and cellular morphology was examined by cytospin slide staining with Giemsa (a). Original magnification ×1000. AG490 alone (5 μM) had no effect on the morphology of the cells. Cellular proliferation was measured by MTT assay, and results are expressed as the means of triplicate experiments (b), and cellular differentiation was assayed by the expression of CD11b antigen using FACS analysis (c). Error bars represent the s.d. from experimental points in triplicate. A combination of As_2O_3 and GM-CSF induced inhibition of cellular proliferation and induced differentiation of UF-1 cells. However, the combination of AG490 (20 μM), As_2O_3 and GM-CSF induced apoptosis of UF-1 cells.

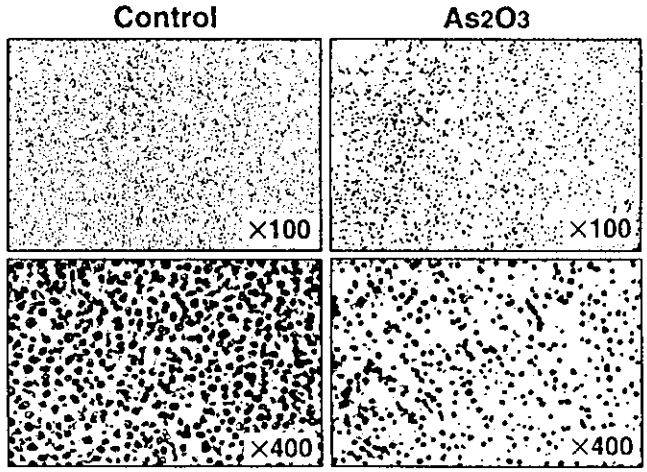

Figure 6 As_2O_3-mediated apoptosis of APL cells *in vivo* using NOD/SCID mice. UF-1 cells (1×10^7 cells) were inoculated subcutaneously into the NOD/SCID mice. Forty days after transplantation, As_2O_3 (9.43 mg/kg body weight) or PBS as a control was injected for 21 days. Tissue was fixed with 4% paraformaldehyde and stained with hematoxylin and eosin. Results for control (left panel) and As_2O_3-treated (right panel) mice are shown. Original magnification ×100 (upper panel) and ×400 (lower panel).

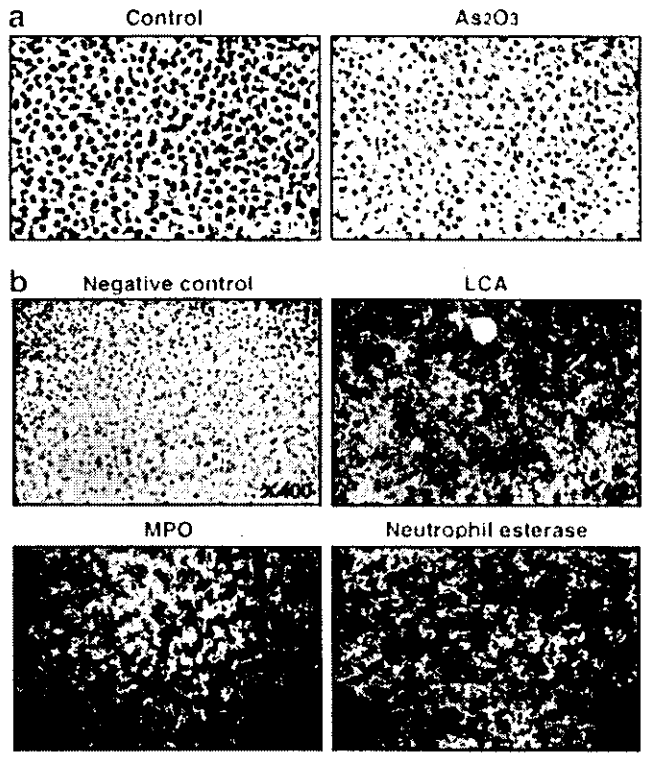

Figure 7 As_2O_3 in combination with GM-CSF induced differentiation of APL cells *in vivo*. (a) The tumor sections from hGM-CSF producing transgenic SCID (hGMTgSCID) mice were fixed in 4% paraformaldehyde, embedded in paraffin, and stained with hematoxylin and eosin. PBS-injected control (left panel) and As_2O_3-treated (right panel) mice. Original magnification ×400. (b) Immunohistological staining. The tumor was frozen in OCT-compound and stained with rabbit anti-human LCA, MPO, and neutrophil esterase antibodies. The spleens of PBS-treated control mice were stained with anti-LCA antibody as a negative control. Original magnification ×1000.

tological studies suggest that these granulocytes were differentiated from the inoculated UF-1 cells.

Discussion

All-*trans* RA has been shown to achieve complete remission in nearly all patients with APL by selectively targeting the oncogenic PML/RARα protein and thereby inducing differentiation of leukemic cells.[5–10] Despite an initial response, APL cells eventually develop resistance to RA, and thus relapse occurs in patients who are treated with RA alone.[11,12] Therapeutic strategies at overcoming resistance to all-*trans* RA are currently being studied. New promising agents that include 9-*cis* RA, a novel synthetic retinoid, Am80, and a liposomal all-*trans* RA have been introduced for refractory APL.[31–33] Developing these approaches has just begun, however, there have been no reliable clinical data for relapsed or RA-resistant APL patients. Therefore, clinical resistance to all-*trans* RA poses a serious problem for differentiation-inducing therapy. Recent clinical investigations in China and the US have shown that As_2O_3 is an effective treatment for patients with APL, even for those who have relapsed after RA-induced clinical remission.[13–17] As_2O_3 initially seems to be a tolerable drug, but recent studies have observed several serious clinical side-effects, including hepatic damage and cardiac dysfunctions, as well as symptoms similar to those of retinoic acid syndrome, a lethal complication of all-*trans* RA which itself manifests like acute respiratory distress syndrome (ARDS).[14,15] In fact, Niu *et al*[15] have reported that seven of 11 (63.6%) newly diagnosed and 15 of 47 (31.9%) relapsed cases of APL were complicated by hepatotoxicity during As_2O_3 treatment, and that two of these patients died of high sGPT and sGPT levels. There is thus need for a new and safer approach to As_2O_3 treatment of patients with RA-resistant APL. We demonstrated in the present study that a combination of As_2O_3 and GM-CSF induced differentiation, but not apoptosis, in APL cells both *in vitro* and *in vivo*.

Although clinical applications have not been extensively examined, *in vitro* studies have shown that induction of differentiation of PML/RARα-positive cells by all-*trans* RA can be enhanced with G-CSF.[5,34] Because these studies have suggested that hematopoietic growth factors may alter the signaling pathway of As_2O_3, we here examined the effects of GM-CSF on As_2O_3-induced apoptosis in both RA-sensitive and -resistant APL cells. Interestingly, a combination of GM-CSF and As_2O_3 could induce differentiation of both NB4 and UF-1 APL cell lines as well as primary APL cells. A double dominant-negative model involving the PML/RARα fusion protein has been proposed to explain the pathogenesis of APL; in this model, PML/RARα blocks the function of wild-type RARα and wild-type PML proteins.[35] Investigations indicate that PML/RARα may be a common target for both RA and As_2O_3, and that both agents lead to a loss of PML/RARα chimeric protein.[6,17] As previously reported,[16] we have demonstrated that As_2O_3 rapidly degrades the PML/RARα protein in both NB4 and UF-1 cells. GM-CSF alone did not change the expression of PML/RARα in the present study but a combination of As_2O_3 and GM-CSF reduced expression of the chimeric protein. These results suggest that PML/RARα degradation or reduction is required for both the induction of apoptosis by As_2O_3 or differentiation by As_2O_3 in combination with GM-CSF in APL cells. In our case, reduction in the expression of the APL-specific PML/RARα fusion protein in response to treatment with As_2O_3 and GM-CSF may have preceded any further differentiation program in APL cells.

Previously published works have suggested that activation of the Ras-Raf-MAP kinase pathway is essential for inhibition of apoptosis following GM-CSF stimulation of neutrophils.[36–38] GM-CSF receptor has been thought to transmit its regulatory signals primarily by the receptor-associated Jak tyrosine kinases. Jak kinases subsequently activate STAT transcription factors and transduce their signals into the nucleus to modulate gene expression.[25,26] It has been reported that Jak2 kinase plays a critical role in GM-CSF-mediated prevention of eosinophil apoptosis.[29] In addition, many investigators have reported that the activation of Jak kinases via cytokine receptors are considered to be anti-apoptotic effects in hematopoietic cells (39). In this study, we showed that GM-CSF alone or a combination of As_2O_3 and GM-CSF can protect apoptosis. We demonstrated that a combination of As_2O_3 and GM-CSF induced activation of Jak2 kinase. AG490, a specific inhibitor of Jak2 kinase, completely blocked the ability of GM-CSF to prevent apoptosis. Moreover, As_2O_3 decreased the expression of activated Jak2 in both NB4 and UF-1 cells, suggesting that Jak2 might be important for the survival of APL cells. In fact, it has been reported that Jak2 kinase is necessary for STAT activation by GM-CSF receptor and is required for cellular proliferation.[25] Therefore, the Jak-STAT pathway is critical for the anti-apoptotic activity of GM-CSF in APL cells treated with a combination of As_2O_3 and GM-CSF. Further studies will be needed to clarify the more detailed molecular mechanisms of the differentiation process in APL cells.

To develop novel therapeutic approaches, a suitable *in vivo* model for human APL is needed, and thus several transgenic mouse models have been developed for the PML/RARα chimeric gene.[40–42] Ten to 20% of the mice derived from PML/RARα transgenic mice using either human cathepsin-G or a human migration inhibitory factor-related protein expression vector developed APL-like leukemia followed by myeloproliferative disorders.[40–42] Because such transgenic approaches require a long period of time to produce APL mice, we previously inoculated RA-resistant UF-1 cells into human GM-CSF-producing transgenic (hGMTg) SCID mice and used these mice to produce an RA-resistant APL mouse model.[21] Since hGMTg SCID mice have a high amount of human GM-CSF in their sera,[20] we reasoned that the combined effects of As_2O_3 and GM-CSF could be examined *in vivo* by means of simple As_2O_3 administration. Using this mouse model, we have demonstrated that As_2O_3 can suppress the growth of subcutaneous tumors by inducing differentiation of UF-1 cells in the presence of GM-CSF *in vivo*.[23] In addition, we have confirmed that As_2O_3 alone can induce apoptosis in UF-1 cells *in vivo* by means of a NOD/SCID mouse model not possessing endogenous human GM-CSF. Thus a combination of As_2O_3 and GM-CSF induces differentiation of APL cells both *in vitro* and *in vivo*. To date, As_2O_3 has been used as a single agent for principally relapsed or RA-resistant APL patients.[13,14] Recent studies have reported that a combination of As_2O_3 and all-*trans* RA enhances differentiation and apoptosis in As_2O_3-resistant NB4 cells *in vitro*,[43] and synergistically eradicates leukemic cells in a transgenic mouse model of APL.[44] The synergism between As_2O_3 and all-*trans* RA could provide us with a novel therapeutic approach for APL. Likewise, the present combination could also lead to a novel clinical approach and should be assessed further in APL patients.

In conclusion, a combination of As_2O_3 and GM-CSF can provide a novel approach for differentiation-inducing therapy in patients with APL.

Acknowledgements

This work was supported by grants from the Ministry of Education, Science and Culture in Japan, and by a National Grant-in-Aid for the Establishment of a High-Tech Research Center in a Private University.

References

1 Kakizuka A, Miller WH Jr, Umesono K, Warrell RP Jr, Frankel SR, Murty VVVS, Dmitrovsky E, Evans RM. Chromosomal translocation t(15;17) in human acute promyelocytic leukemia fuses RARα with a novel putative transcription factor, PML. *Cell* 1991; **66**: 663–674.
2 de Thé H, Lavau C, Marchio A, Chomienne C, Degos L, Dejean A. The PML-RAR alpha fusion mRNA generated by the t(15;17) translocation in acute promyelocytic leukemia encodes a functionally altered RAR. *Cell* 1991; **66**: 675–684.
3 Grignani F, Ferrucci PF, Testa U, Talamo G, Fagioli M, Alcalay M, Mencarelli A, Grignani F, Peschle C, Nicoletti I. The acute promyelocytic leukemia specific PML/RARα protein inhibits differentiation and promotes survival of myeloid precursor cells. *Cell* 1993; **74**: 423–431.
4 Grignani F, Testa U, Fagioli M, Barkeri T, Masciulli R, Marinari G, Peschle C, Pelicci PG. Promyelocytic leukemia-specific PML-retinoic acid alpha receptor fusion protein interferes with erythroid differentiation of human erythroleukemia K562 cells. *Cancer Res* 1995; **55**: 440–443.
5 Raelson JV, Nervi C, Rosenauer A, Benedetti L, Monczak Y, Pearson M, Pelicci PG, Miller WH. PML/RARα oncoprotein is a direct molecular target of retinoic acid in acute promyelocytic leukemia cells. *Blood* 1996; **88**: 2826–2832.
6 Yoshida H, Kitamura K, Tanaka K, Omura S, Miyazaki T, Hachiya T, Ohno R, Naoe T. Accelerated degradation of PML-retinoic acid receptor α (PML-RARα) oncoprotein by all-*trans*-retinoic acid in acute promyelocytic leukemia: possible role of the protease pathway. *Cancer Res* 1996; **56**: 2945–2948.
7 Huang ME, Ye YC, Chen SR, Chai JR, Lu JX, Zhoa L, Gu HT, Wang ZY. Use of all-*trans* retinoic acid in the treatment of acute promyelocytic leukemia. *Blood* 1988; **72**: 567–572.
8 Castaigne S, Chomienne C, Daniel MT, Ballarini P, Berger R, Fenauz P, Degos L. All-*trans* retinoic acid as a differentiation therapy for acute promyelocytic leukemia. I. Clinical results. *Blood* 1990; **76**: 1704–1709.
9 Warrell RP Jr, Frankel SR, Miller WH Jr, Sheinberg DA, Itri LM, Hittelman WN, Vyas R, Andreeff M, Tafuri A, Jakubowski A, Gabrilove J, Gordon MS, Dmitrovsky E. Differentiation therapy of acute promyelocytic leukemia with tretinoin (all-*trans*-retinoic acid). *N Engl J Med* 1991; **324**: 1385–1393.
10 Kanamaru A, Takemoto Y, Tanimoto M, Murakami H, Asou N, Kobayashi T, Kuriyama K, Ohmoto E, Sakamaki H, Tsubaki K, Hiraoka H, Yamada O, Oh H, Saito K, Matsuda S, Minato K, Ueda T, Ohno R. All-*trans* retinoic acid for the treatment of newly diagnosed acute promyelocytic leukemia. *Blood* 1995; **85**: 1202–1206.
11 Warrell RP Jr. Retinoid resistance in acute promyelocytic leukemia: New mechanisms, strategies, and implications. *Blood* 1993; **82**: 1941–1953.
12 Kizaki M, Ueno H, Matsushita H, Takayama N, Muto A, Awaya N, Ikeda Y. Retinoid resistance in leukemic cells. *Leuk Lymphoma* 1997; **25**: 427–434.
13 Shen ZX, Chen GQ, Ni JH, Li XS, Xiong SM, Qui QY, Zhu J, Tang W, Sun GL, Yang KQ, Chen Y, Zhou L, Fang ZW, Wang YT, Ma J, Zhang P, Zhang TD, Chen SJ, Chen Z, Wang ZY. Use of arsenic trioxide (As_2O_3) in the treatment of acute promyelocytic leukemia (APL): II. Clinical efficiency and pharmacokinetics in relapsed patients. *Blood* 1997; **89**: 3354–3360.
14 Soignet SL, Maslak P, Wang ZG, Thanwar S, Calleja E, Dardashti LJ, Corso D, DeBlasio A, Gabrilove J, Scheinberg DA, Pandolfi RP, Warrell RP Jr. Complete remission after treatment of acute promyelocytic leukemia with arsenic trioxide. *N Engl J Med* 1998; **339**: 1341–1348.
15 Niu C, Yan H, Yu T, Sun HP, Liu JX, Li XS, Wu LW, Zhang FQ, Chen Y, Zhou L, Li JM, Zeng XY, Yang RRO, Yuan MM, Ren MY, Gu FY, Cao Q, Gu BW, Su XY, Chen GQ, Xiong SM, Zhang TD, Waxman S, Wang ZY, Chen Z, Hu J, Shen ZX, Chen SJ. Studies on treatment of acute promyelocytic leukemia with arsenic trioxide: remission induction, follow-up, and molecular monitoring in 11 newly diagnosed and 47 relapsed promyelocytic leukemia patients. *Blood* 1999; **94**: 3315–3324.
16 Chen GQ, Zhu J, Shi XG, Ni JH, Zhong HJ, Si GY, Jin XL, Tang W, Li XS, Xong SM, Shen ZX, Sun GL, Ma J, Zhang P, Zhang TD, Gazin C, Naoe T, Chen SJ, Wang ZY, Chen Z. *In vitro* studies on cellular and molecular mechanisms of arsenic trioxide (As_2O_3) in the treatment of acute promyelocytic leukemia: As_2O_3 induces NB4 cell apoptosis with downregulation of bcl-2 expression and modulation of PML-RARα/PML proteins. *Blood* 1996; **88**: 1052–1061.
17 Shao W, Fanelli M, Ferrara FF, Riccioni R, Rosenauer A, Davison K, Lymph WW, Waxman S, Pelicci PG, Lo Coco F, Avvisati G, Testa U, Peschle C, Gambacorti-Passerini C, Nervi C, Miller WH Jr. Arsenic trioxide as an inducer of apoptosis and loss of PML/RARα protein in acute promyelocytic leukemic cells. *J Natl Cancer Inst* 1998; **90**: 124–133.
18 Wang ZG, Rivi R, Delva L, Konig A, Scheinberg DA, Gambacorti-Passerini C, Bagrilove JL, Warrell RP, Pandolfi RP. Arsenic trioxide and melarsoprol induce programmed cell death in myeloid leukemia cell lines and function in a PML and PML-RARα independent manner. *Blood* 1998; **92**: 1497–1504.
19 Kizaki M, Matsushita H, Takayama N, Muto A, Ueno H, Awaya N, Kawai Y, Asou H, Kamada N, Ikeda Y. Establishment and characterization of a novel acute promyelocytic leukemia cell line (UF-1) with retinoic acid-resistant features. *Blood* 1996; **88**: 1824–1833.
20 Miyakawa Y, Fukuchi Y, Ito M, Kobayashi K, Kuramoto T, Ikeda Y, Takeda Y, Yanaka T, Miyasaka M, Nakahata T, Tamaoki N, Nomura T, Ueyama Y, Shimamura K. Establishment of human granulocyte–macrophage colony stimulating factor producing transgenic SCID mice. *Br J Haematol* 1996; **95**: 437–442.
21 Fukuchi Y, Kizaki M, Kinjo K, Awaya N, Ito M, Kawai Y, Umezawa A, Hata J, Ueyama Y, Ikeda Y. Establishment of a retinoic acid-resistant human acute promyelocytic leukemia (APL) model in human granulocyte–macrophage colony-stimulating factor (GM-CSF) transgenic severe combined immunodeficiency (SCID) mice. *Br J Cancer* 1998; **78**: 878–884.
22 Kizaki M, Muto A, Kinjo K, Ueno H, Ikeda Y. Application of heavy metal and cytokine for differentiation-inducing therapy in acute promyelocytic leukemia. *J Natl Cancer Inst* 1998; **10**: 1906–1907.
23 Kinjo K, Kizaki M, Muto A, Fukuchi Y, Umezawa K, Yamato K, Nishihara T, Hata J, Ito M, Ueyama Y, Ikeda Y. Arsenic trioxide (As_2O_3)-induced apoptosis and differentiation in retinoic acid-resistant acute promyelocytic leukemia model in hGM-CSF-producing transgenic SCID mice. *Leukemia* 2000; **14**: 431–438.
24 Dong JT, Luo XM. Effects of arsenic on DNA damage and repair in human fetal lung fibloblasts. *Mutat Res* 1994; **315**: 11–15.
25 Blalock WL, Weinstein-Oppenheimer C, Chang F, Hoyle PE, Wang X-Y, Algate PA, Franklin RA, Oberhaus SM, Steelman LS, McCubrey JA. Signal transduction, cell cycle regulatory, and anti-apoptotic pathways regulated by IL-3 in hematopoietic cells: possible sites for intervention with anti-neoplastic drugs. *Leukemia* 1999; **13**: 1109–1166.
26 McCubrey JA, May WS, Duronio V, Mufson A. Serine/threonin phosphorylation in cytokine signal transduction. *Leukemia* 2000; **14**: 9–21.
27 Lanotte M, Martin-Thouvenin V, Najman S, Balerini P, Valensi F, Berger R. NB4, a maturation inducible cell line with t(15;17) marker isolated from a human acute promyelocytic leukemia (M3). *Blood* 1991; **77**: 1080–1086.
28 Workman P, Balmain A, Hickman JA, McNally NJ, Mitchison NA, Pirepoint CG, Raymond G, Rowlatt C, Stephens TC, Wallace J. UKCCCR guidelines for the welfare of animals in experimental neoplasia. *Br J Cancer* 1998; **58**: 109–113.
29 Simon HU, Yousefi S, Dibbert B, Levi-Scaffer F, Blasser K. Anti-apoptotic signals of granulocyte–macrophage colony-stimulating factor are transduced via Jak2 tyrosine kinase in eosinophils. *Eur J Immunol* 1997; **27**: 3536–3539.
30 Sakai I, Kraft AS. The kinase domain of Jak2 mediates induction

of Bcl-2 and delays cell death in hematopoietic cellc. *J Biol Chem* 1997; **272**: 12350–12358.

31 Fenaux P, Chomienne C, Degos L. Acute promyelocytic leukemia: biology and treatment. *Semin Oncol* 1997; **24**: 92–102.

32 Lo Coco F, Nervi C, Avvisati G, Mandelli F. Acute promyelocytic leukemia: a curable disease. *Leukemia* 1998; **12**: 1866–1880.

33 Douer D, Estey E, Santillana S, Bennett JM, Lopez-Bernstein G, Boehm K, Williams T. Treatment of newly diagnosed and relapsed acute promyelocytic leukemia with intravenous liposomal all-*trans* retinoic acid. *Blood* 2001; **97**: 73–80.

34 Nakamaki T, Sakashita A, Sano M, Hino K, Suzuki K, Tomoyasu S, Tsuruoka N, Honma Y, Hozumi M. Granulocyte colony-stimulating factor and retinoic acid cooperatively induce granulocytic differentiation of acute promyelocytic leukemia cells *in vitro*. *Jpn J Cancer Res* 1989; **80**: 1077–1082.

35 Quignon F, Chen Z, de Thé H. Retinoic acid and arsenic: towards oncogene-target treatment of acute promyelocytic leukemia. *Biochem Biophys Acta* 1997; **1333**: M53-M61.

36 Yousefi S, Hoessli DC, Blaser K, Mills GB, Simon HU. Requirement of Lyn and Syk tyrosine kinases for the prevention of apoptosis by cytokines in human eosinophils. *J Exp Med* 1996; **183**: 1407–1414.

37 Wei S, Liu JH, Epling-Burnette PK, Gameto AM, Ussery D, Pearson EW, Elkabani ME, Diaz JL, Djeu JY. Critical role of Lyn kinase in inhibition of neutrophil apoptosis by granulocyte-macrophage colony-stimulating factor. *J Immunol* 1996; **157**: 5155–5162.

38 McCubrey JA, Steelman LS, Hoyle PA, Blalock WL, Weinstein-Oppenheimer CR, Franklin RA, Cherwinski H, Bosch E, McMahon M. Differential abilities of activated Raf oncoproteins to abrogate cytokine dependency, prevent apoptosis and induce autocrine growth factor synthesis in human hematopoietic cells. *Leukemia* 1998; **12**: 1903–1929.

39 Franklin RA, McCubrey JA. Kinases: positive and negative regulators of apoptosis. *Leukemia* 2000; **14**: 2019–2034.

40 He LZ, Tribioli C, Rivi R, Peruzzi D, Pelicci PG, Soares V, Cattoretti C, Pandolfi RP. Acute leukemia with promyelocytic features in PML/RARα transgenic mice. *Proc Natl Acad Sci USA* 1997; **94**: 5302–5307.

41 Grisolano JL, Wesselschmidt RL, Pelicci PG, Ley TJ. Altered myeloid development and acute leukemia in transgenic mice expressing PML-RARα under control of cathepsin G regulatory sequences. *Blood* 1997; **89**: 376–387.

42 Brown D, Kogan S, Lagasse E, Weissman L, Alcalay M, Pelicci PG, Atwater S, Bishop JM. A PMLRARα transgene initiate murine promyelocytic leukemia. *Proc Natl Acad Sci USA* 1998; **94**: 2551–2556.

43 Gianni M, Koken MHM, Chelbi-Alix MK, Benoit G, Lanotte M, Chen Z, de Thé H. Combined arsenic and retinoic acid treatment enhances differentiation and apoptosis in arsenic-resistant NB4 cells. *Blood* 1998; **91**: 4300–4310.

44 Lallemand-Breitenbach V, Guillemin MC, Janin A, Daniel MT, Degos L, Kogan SC, Bishop JM, de Thé H. Retinoic acid and arsenic synergize to eradicate leukemic cells in a mouse model of acute promyelocytic leukemia. *J Exp Med* 1999; **189**: 1043–1052.

Experimental Cell Research 266, 114–125 (2001)
doi:10.1006/excr.2001.5203, available online at http://www.idealibrary.com on IDEAL®

EAT/mcl-1 Expression in the Human Embryonal Carcinoma Cells undergoing Differentiation or Apoptosis

Makoto Sano,* Akihiro Umezawa,*,[1] Hitoshi Abe,* Akira Akatsuka,† Shuko Nonaka,‡ Hiroshi Shimizu,‡,§ Mariko Fukuma,* and Jun-ichi Hata*

*Department of Pathology and ‡Department of Dermatology, Keio University School of Medicine, 35 Shinanomachi, Shinjuku-ku, Tokyo, 160-582, Japan; †Laboratory for Structure and Function Research, Tokai University School of Medicine, Bohseidai, Isehara-shi, Kanagawa, 259-1193, Japan; and §Department of Dermatology, Hokkaido University School of Medicine, North 15, West 7, Kita-ku, Sapporo 060-8638, Japan

Differentiation and apoptosis are precisely regulated events in early embryogenesis. Retinoic acid-induced differentiation in the embryonal carcinoma (EC) cell line NCR-G3 triggers concurrent induction of apoptosis. Using this system, which serves as a model of early embryogenesis, the expression of various bcl-2-related genes was analyzed as these genes display either positive or negative regulatory effects on apoptosis. EAT/mcl-1, an antiapoptotic bcl-2-related gene and immediate early gene, was dramatically expressed at an early stage of NCR-G3 differentiation. Bcl-xL, another antiapoptotic gene, was induced at a middle stage of differentiation and then gradually decreased to basal level. Expression of Bax, a proapoptotic molecule, was detected at a high level and remained relatively constant. Meanwhile, Bcl-2 and Bcl-xS were below detectable levels throughout the various stages of differentiation. As the balance of bcl-2 genes is a crucial regulatory step in apoptosis, the results suggest that EAT and Bax likely regulate apoptosis in the early stages of differentiation. In later stages of differentiation, down-regulation of EAT was found to coincide with a gradual increase in apoptosis of NCR-G3 cells. Furthermore, use of the monoclonal antibody (3A2) specific to EAT revealed that EAT is localized to the outer mitochondrial membrane in human EC cells. In addition, EAT immunoreactivity was not detected in apoptotic NCR-G3 cells while it was observed in nearly all viable cells. The findings suggest that rapid induction of EAT may prevent NCR-G3 cells from undergoing apoptosis, thereby supporting viability at the early stage of differentiation. © 2001 Academic Press

Key Words: **human EC cells; differentiation; apoptosis EAT/mcl-1; bcl-2 family; monoclonal antibody; cDNA array.**

INTRODUCTION

Early human embryogenesis is chronicled by a well-regulated sequence of cell differentiation events and is likewise correlated with regulated removal of unnecessary cells by apoptosis. A model of early human embryonic development has been established by the use of embryonal carcinoma (EC) cell lines [1–3]. NCR-G3 cells were established from a human testicular mixed EC and are able to differentiate into neuronal, myogenic, and epithelial as well as the trophectodermal lineage upon exposure to retinoic acid (RA) or heat shock [4, 5]. RA-induced differentiation in NCR-G3 cells has been established to also trigger a concurrent induction in apoptosis [6].

Apoptosis is genetically programmed cell death and is characterized by morphological features such as chromatin condensation, plasma membrane blebbing, cell shrinkage, and nuclear fragmentation. However, prior to the appearance of these morphological features, the mitochondrial transmembrane potential collapses, initiating the early stage of apoptosis [7]. Sequentially, the outer mitochondrial membrane is physically disrupted [8], followed by release of cytochrome *c* or apoptosis-initiating factors from the mitochondrial intermembrane space to the cytosol [9, 10]. These proteins of the mitochondrial intermembrane space are implicated in the activation of caspases, thereby initiating and executing the morphological changes of apoptosis. Thus, the mitochondria is an important organelle regulating the early stages of the apoptotic pathway. Bcl-2-related proteins have been shown to localize mainly in the outer mitochondrial membrane [11, 12] and to modulate mitochondrial permeability [13]. These important functions are believed to initiate the apoptotic mechanism.

EAT/mcl-1 (EAT), which encodes a bcl-2-related protein, was originally isolated as a gene whose expression is induced at an early stage of differentiation in NCR-G3 cells [14]. It has since been found to inhibit

[1] To whom correspondence and reprint requests should be addressed. Fax: +81-3-3353-3290. E-mail: au@med.keio.ac.jp.

0014-4827/01 $35.00

apoptosis under a variety of apoptosis-inducing conditions [15–18]. The human EAT gene was found to be identical in sequence with mcl-1, a member of the bcl-2 family, which was isolated from a human myeloid leukemia cell line during TPA-induced differentiation into the monocyte/macrophage lineage [19]. The murine orthologue of the EAT gene has also been isolated and has been established to be similarly induced by RA in murine embryonic stem (ES) cells and murine EC cell lines such as TT2, PCC3, and F9 [20]. The presence of a differential splicing variant, mcl-1s (EAT splicing variant), has recently been reported to promote cell death [21, 22]. The variant results from skipping of the second exon and thus remains BH3 domain only, but not BH1, BH2, and transmembrane-encoding domains. Therefore, the full-length EAT functions to enhance cell survival, while the EAT splicing variant promotes cell death. Full-length EAT is more abundant than the EAT splicing variant in most cells.

EAT is also known to be an immediate early gene that has an immediate response box in its 3′-untranslated region like other immediate early genes such as c-*fos*, c-*jun*, and colony-stimulation factor-1 [20]. This evidence implicates a role for EAT in the cellular differentiation associated with embryogenesis. However, the precise expression pattern and intracellular localization during EC differentiation have not been elucidated. We used the monoclonal antibody which reacts specifically to EAT and determined the localization of EAT in a human EC cell line. Furthermore, we investigated the expression of bcl-2-related proteins in EC cells undergoing differentiation or apoptosis.

MATERIALS AND METHODS

Monoclonal antibody, 3A2, to human EAT. A cDNA-encoding human EAT, corresponding to amino acids 31 to 229, was inserted into the pGEX-2T expression vector (Pharmacia Biotech, Uppsala, Sweden). This plasmid was transformed into a protease-deficient strain of *Escherichia coli* (BL21). The GST–EAT fusion protein was overexpressed by adding 0.5 mM isopropyl-β-D-thiogalactoside and lysed in PBS containing 10 mM dithiothreitol and followed by purification with chromatography on glutathione–Sepharose 4B (Pharmacia Biotech). Female BALB/c mice (6 weeks old) were immunized with 300 μg of the purified fusion protein conjugate in Freund's complete adjuvant via intraperitoneal injections, followed by two additional immunizations with the immunogen in incomplete adjuvant at an interval of 2 weeks. For final boosting, the mice were intravenously immunized with about 50 μg of purified fusion protein. Thus, in total, four immunizations were carried out. Four days after final boosting, the immune splenocytes were fused with NS1/1-Ag4-1. Approximately 5×10^6 hybridoma cells were injected into pristane-pretreated female BALB/c nude mice (6 weeks old) intraperitoneally. Murine ascites was purified by affinity chromatography on protein G–Sepharose (Pharmacia Biotech). The immunoglobulin subclass was determined with a mouse monoclonal antibody isotyping kit (Amersham, Buckinghamshire, UK).

The specificity of 3A2 antibody (IgG1) was tested by immunoblot analysis (Fig. 1A). The 3A2 antibody reacted with a band representing a 50-kDa GST–EAT fusion protein, but not the expected 29-kDa GST band. The (10)1-EAT and (10)1-neo cells are transfected with full-length EAT cDNA or neomycin-resistance gene, respectively [15], and the presence of EAT protein was tested. The 3A2 antibody detected the approximately 40-kDa full-length EAT protein in (10)1-EAT cells, but did not react with the (10)1-neo cell lysates. The 40-kDa EAT band was blocked by preincubation with the GST–EAT fusion protein against 3A2 antibody, but not by addition of GST protein. Furthermore, immunocytochemical analysis revealed EAT immunoreactivity in the (10)1-EAT cells, but not in the (10)1-neo cells (Fig. 1B), indicating that 3A2 antibody reacts specifically with human EAT. The experiments used with the 3A2 antibody have been previously reported [15, 23].

Cell culture. NCR-G3, a human embryonal carcinoma cell line, was cultured in a 1:1 mixture of Dulbecco's modified Eagle's medium and Ham's F12 medium supplemented with 10% fetal calf serum. The NCR-G3 cells were differentiated with exposure to 5×10^{-5} M all-*trans*-RA as described previously [14]. A murine p53-deficient fibroblast cell line, (10)1, was cultured in Dulbecco's modified Eagle medium supplemented with 10% fetal calf serum [15].

Immunoblotting. Cells were washed with cold PBS and lysed by suspension in triple detergent lysis buffer (150 mM NaCl, 0.02% sodium azide, 0.1% SDS, 1% NP-40, 0.5% sodium deoxycholate, 100 μg/ml PMSF, and 1 μg/ml aprotinin in 50 mM Tris–HCl, pH 8.0). After addition of sample buffer (10% glycerol, 2.3% SDS, and 5% β-mercaptoethanol in 62.5 mM Tris–HCl, pH 6.8) to achieve an equivalent sample volume, the resulting suspension was boiled for 2 min. The lysates were loaded onto 10–12.5% SDS–polyacrylamide gel. After SDS–PAGE, proteins were transferred electrophoretically onto polyvinylidene difluoride (PVDF) membrane. The membranes were blocked for 1 h with 5% nonfat dried milk in TBS-T (0.1% Tween 20 and 137 mM NaCl in 20 mM Tris–HCl, pH 7.6). They were incubated for 1 h with primary antibody diluted at 1:1000 in blocking solution and rinsed with TBS-T. After incubation with horseradish peroxidase (HRP)-conjugated rabbit anti-mouse immunoglobulin or swine anti-rabbit immunoglobulin diluted at 1:1000 in blocking solution, immunoreactivities were visualized with enhanced chemiluminescence reagents (Amersham). To detect bcl-2 family members, immunoblotting was performed with antibodies against EAT (3A2 monoclonal antibody, described above and rabbit polyclonal antibody, $\alpha EAT_{31\text{-}229}$ [24]), Bcl-2, Bcl-x (Santa Cruz Biotechnology Inc., Santa Cruz, CA), and Bax (Chemicon International Inc., Temecula, CA). The presence of cytochrome *c* oxidase (complex IV) (COX-IV) was analyzed with A-6431 monoclonal antibody (Molecular Probes, Inc., Leiden, The Netherlands).

Immunostaining. Cells attached to Lab-Tek chamber slides (Nunc, Inc., Naperville, IL) were washed with serum-free medium. Floating cells were cytocentrifuged onto poly-L-lysine-coated glass slides. Cells were dried immediately and fixed with acetone for 15 min. After washing with PBS, they were preblocked for 1 h with 1% bovine serum albumin (BSA) and 5% normal rabbit serum in PBS and then incubated overnight at 4°C with 3A2 antibody diluted at 1:500 in 1% BSA–PBS. After incubation with HRP-conjugated rabbit anti-mouse immunoglobulin diluted at 1:100, cells were washed in PBS. Staining was developed using a solution containing 3,3′-diaminobenzidine (DAB), 0.01% H_2O_2, and 10 mM sodium azide in 0.05 M Tris–HCl buffer, pH 7.6. Slides were counterstained with methyl green.

RT (reverse transcription)–PCR detection of EAT in NCR-G3 cells. Isolation of total RNA from cells was performed using RNEasy spin column kits (Qiagen, Chatsworth, CA) according to the manufacturer's instruction. cDNAs were synthesized from 5 μg total RNAs with first-strand cDNA synthesis kit (Amersham Pharmacia Biotech, Uppsala, Sweden). The primers used for EAT were 5′-AGGAATTCGATGTTTGGCCTCAAAAGAAACGCGGTA-3′ and 5′-GAATTCGGAAGTTACAGCTTGGAGTCCAACTGC-3′ (Life Technologies, Rockville, MD). Each PCR regime involved at 94°C, 1-min initial denaturation step followed by 30 cycles, 61°C for 1 minute (EAT) or

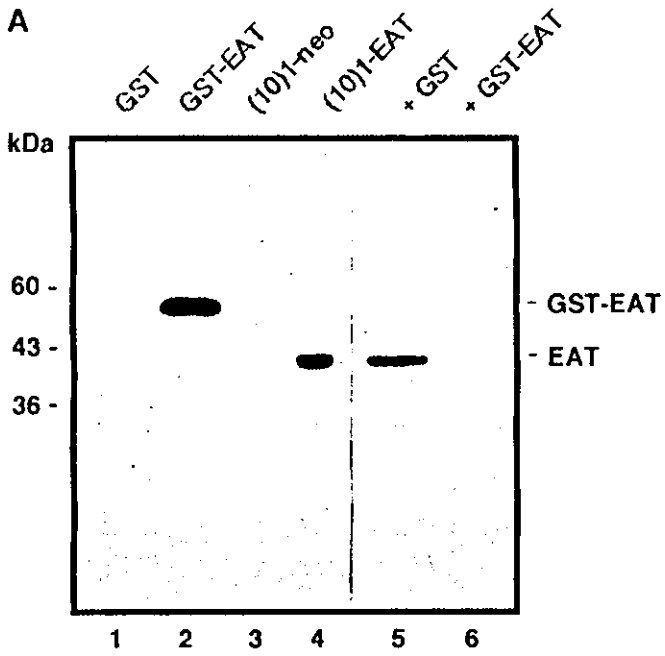

FIG. 1. Specificity of 3A2 monoclonal antibody to human EAT. (A) The specificity of 3A2 antibody was tested by immunoblot analysis. GST (lane 1) and the GST–EAT fusion protein (lane 2) were produced by expression in *Escherichia coli*. (10)1-neo cells (lane 3) and (10)1-EAT cells (lanes 4–6) are transfected with the neomycin-resistance gene or full-length EAT cDNA, respectively. Equal amounts (50 μg) of lysates were loaded on each lane. Immunoblotting was carried out using either 3A2 antibody alone (lanes 1–4) or after preincubation with GST (lane 5) or GST–EAT fusion protein (lane 6). (B) The specificity of 3A2 was also tested by immunocytochemical analysis. Prominent immunoreactivity with 3A2 antibody was detected in the (10)1-EAT cells (b), whereas less immunointensity was seen in the (10)1-neo cells (a).

67°C for 2 min (β-actin), and 72°C for 1 min (EAT) or 2 min (β-actin) on a GeneAmp PCR system 9600 (Applied Biosystems, Foster City, CA). The PCR products were separated by electrophoresis on 1% agarose gels.

RNase protection assay. RNase protection assay was performed according to the manufacturer's instructions (PharMingen, San Diego, CA). RNA was prepared from NCR-G3 cells using Isogen (Waco, Osaka, Japan). The isolated RNA and radiolabeled antisense RNA probes were hybridized at 56°C for 16 h and incubated with RNase for 45 min at 37°C. After digestion with proteinase K, the RNA was extracted with phenol and chloroform, and loaded onto 5% polyacrylamide gel.

Subfractionation of NCR-G3 cells. Cells were washed twice in cold PBS and once in cold hypotonic buffer (2 mM $MgCl_2$ in 10 mM Tris–HCl, pH 7.5). Cells were resuspended in cold hypotonic buffer and homogenized on ice. After centrifugation at 600*g* for 5 min, the sediment of the nuclear fraction was rinsed with 0.25 M sucrose solution (0.25 M sucrose, 2 mM $MgCl_2$, 10 mM Tris–HCl, pH 7.5) and lysed in triple detergent lysis buffer. The supernatant was subjected to additional centrifugation at 9000*g* for 10 min, and the sediment of the intact mitochondrial fraction was rinsed with 0.25 M sucrose solution and lysed in lysis buffer. Microsome represented the sediment from the supernatant after continual centrifugation at 105,000*g* for 1 h. This was rinsed with 0.25 M sucrose solution and lysed in the lysis buffer. The final supernatant yielded the cytosolic fraction.

Alkali extraction and trypsin treatment of intact mitochondria. Intact mitochondria were isolated from RA-exposed NCR-G3 cells by differential centrifugation as described above. The mitochondria were resuspended in freshly prepared 0.1 M Na_2CO_3, pH 11.5, to a final concentration of 0.25 mg/ml and incubated on ice for 30 min with periodic vortexing. Membranes were collected by centrifugation as previously described [25]. Intact mitochondria were also resuspended in PBS containing trypsin (0.2 mg/ml) and incubated on ice for 20 min.

Preembedding immunoelectron microscopy. Cells were fixed in periodate-lysine-paraformaldehyde for 2 h at 4°C. After washing in PBS containing a 5–10% sucrose gradient, cells were frozen for 1 h at −80°C and thawed at room temperature. After inhibition of endogenous peroxidase and incubation with normal sheep serum, the cells were reacted with the anti-human EAT 3A2 monoclonal antibody overnight at 4°C and HRP-conjugated sheep anti-mouse Igs for 3 h at room temperature. The enzyme reaction was performed with 0.02% DAB containing 0.005% H_2O_2 for 2 min. After postfixation with 2% OsO_4, the cells were embedded in Quetol 812 resin for immunoelectron microscopy. Ultrathin sections were examined using a JEOL 1200EX electron microscopy.

Postembedding immunoelectron microscopy. Cells were cryoprotected by soaking in 15% glycerol/PBS and rapidly frozen by plunging into liquid propane, cooled to −190°C, at a speed of 3 m/s, as described previously [26]. Subsequently, the cells were subjected to freeze substitution in 100% acetone for 120 h at −80°C. The temper-

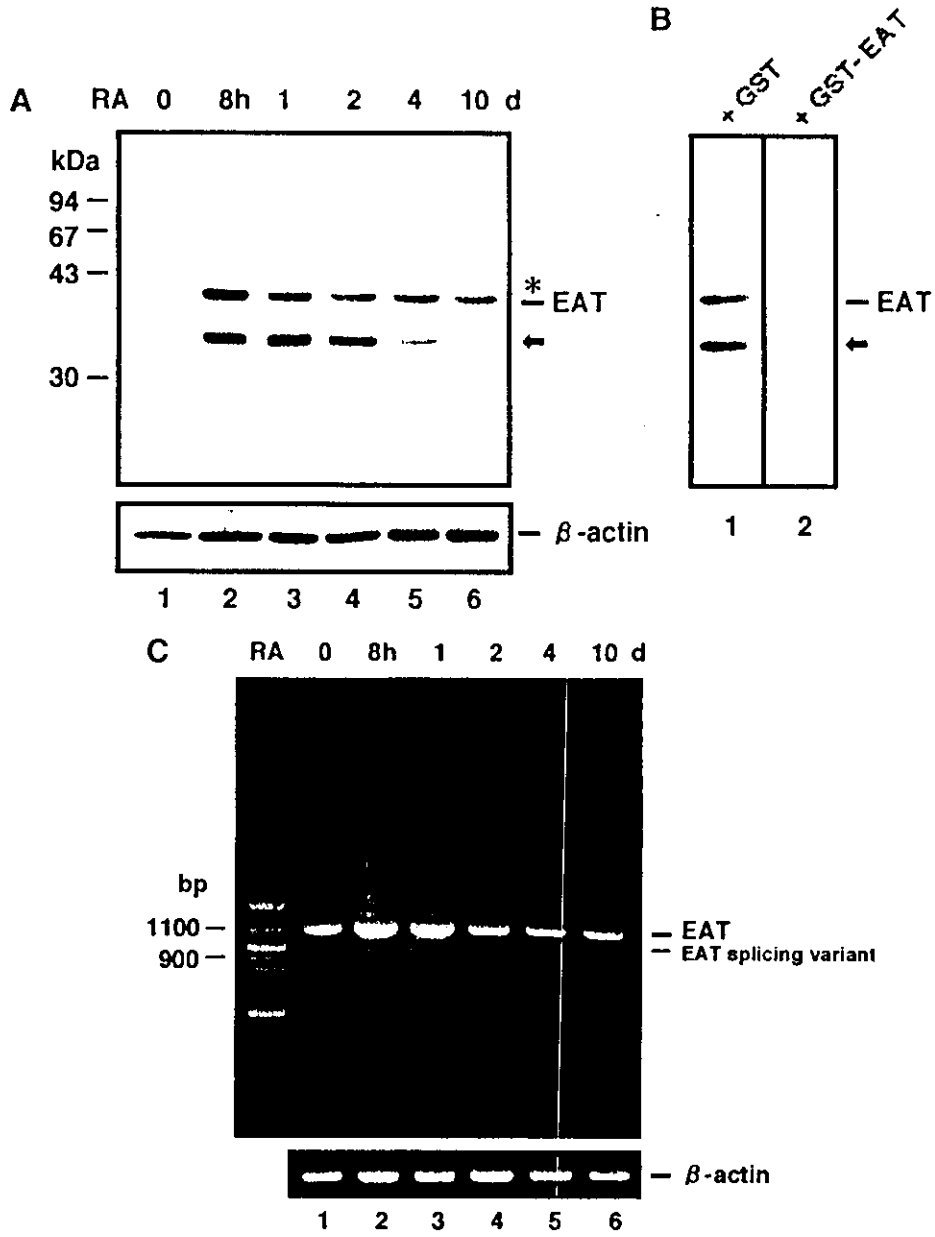

FIG. 2. Induction of EAT in NCR-G3 cells undergoing differentiation. (A) Time course of EAT protein level was analyzed in NCR-G3 undergoing differentiation. NCR-G3 cells were exposed to 5×10^{-5} M RA for the indicated times and assayed for the presence of EAT by immunoblotting with $\alpha EAT_{31\text{-}229}$ antibody (top column). The antibody reacted with 40-kDa EAT and 35-kDa protein specifically (arrow). The expression pattern of EAT was reproducibly observed in separate two experiments. The additional two bands (asterisk) above full-length EAT were blocked neither by phosphatase treatment of lysates nor by preincubation of the antibody with recombinant EAT protein. The expression of β-actin protein was monitored as a loading control (bottom column). (B) NCR-G3 cells were incubated for 8 h in the presence of RA and equal amounts of the lysates were loaded on each lane (lanes 1 and 2). Immunoblotting was carried out with either $\alpha EAT_{31\text{-}229}$ after preincubation with GST (lane 1) or GST–EAT fusion protein (lane 2). The 40-kDa EAT and 35-kDa protein bands were blocked by preincubation with the GST–EAT fusion protein against the antibody, but not by addition of GST protein. (C) The transcripts of a full-length EAT (1155 bp) and the splicing variant (907 bp) prepared from NCR-G3 cells were detected by RT-PCR amplification (top column). NCR-G3 cells were differentiated with exposure to 5×10^{-5} M RA for the indicated times (lanes 1 through 6). The presence of β-actin served as a loading control (bottom column). Molecular weight marker (100 bp ladder) are shown in the left.

ature was raised to −60°C (at a rate of 5°C/h) and the cells were embedded in Lowicryl K11M. Polymerization was initiated under ultraviolet radiation for 48 h at −60°C and continued for an additional 72 h at room temperature. Ultrathin sections collected on the grid were placed on a drop of 5% normal goat serum in 1% BSA–PBS, pH 7.4 for 60 min. After blocking, the sections were incubated in 3A2 monoclonal antibody (1:200) at 4°C overnight. The sections were then placed on goat anti-mouse immunoglobulin conjugated 5 nm

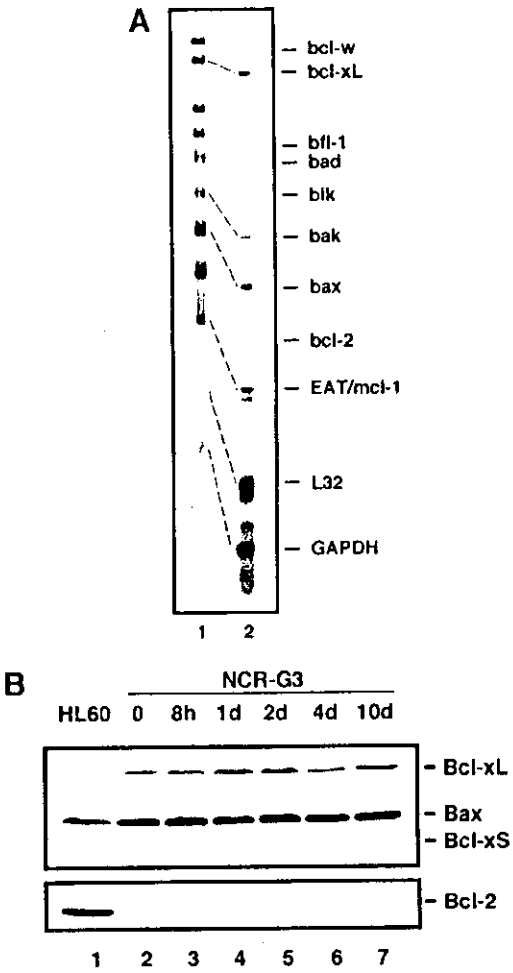

FIG. 3. Expression of bcl-2-related genes in NCR-G3 differentiation. (A) After incubation with 5×10^{-5} M RA for 8 h, expression of members of the bcl-2 family during the NCR-G3 differentiation was determined by RNase protection assay. In the antiapoptotic molecules, EAT and bcl-xL were predominantly expressed in the RA-exposed NCR-G3 cells. Meanwhile, bax was prominently expressed in the pro-apoptotic molecules. (B) NCR-G3 cells were also exposed with RA for the indicated times (lanes 2 through 7) and subjected to SDS–PAGE (12.5%), followed by immunoblotting with antiserum that recognize Bcl-2, Bcl-x, and Bax. HL-60, a human leukemia cell line, served as a positive control for the presence of bcl-2 expression (lane 1).

colloidal gold at a 1:40 dilution at room temperature for 2 h, followed by immunogold silver enhancement [27]. The sections were counterstained with uranyl acetate and lead citrate and observed under a transmission electron microscope (Model 1200EX, JEOL, Tokyo, Japan).

TdT-mediated dUTP–biotin labeling (TUNEL) in frozen section. Cells were fixed in 4% paraformaldehyde for 15 min and washed in PBS containing sucrose. Cell blocks were snap-frozen in OCT compound in a bath of acetone and dry ice. Frozen sections (6 μm) were mounted on PLL-coated glass slides. Expression of the EAT protein was detected by immunostaining using 3A2 antibody as described above. After removal of the methyl green, endogenous biotin and avidin were preblocked with blocking solution (Nichirei, Tokyo, Japan). Nicked DNA ends were labeled at room temperature for 60 min with biotin–dUTP by terminal deoxynucleotide transferase (Boehringer Mannheim). After washing in PBS, slides were incubated with HRP-conjugated streptavidin for 5 min. Staining was developed using a solution containing 3-amino-9-ethylcarbazole, *N,N*-dimethylformamide and H_2O_2 in acetate buffer (Dako Japan Co., Kyoto, Japan).

Flow cytometric analysis. For single-cell suspension, cells were washed in PBS and treated with 0.25% trypsin in PBS containing 0.02% EDTA. The cells were fixed in cold 4% paraformaldehyde for 15 min and washed twice with PBS and refixed in cold acetone for 5 min. After washing in PBS, TUNEL method was performed as described above. Cells were incubated with tetramethylrhodamine isothiocyanate (TRITC)-conjugated streptavidin (Southern Biotechnology, Birmingham, AL) for 30 min on ice (1:50 dilution). Cells were analyzed in a flow cytometer using Epics XL-MCL (Coulter, Hialeah, FL).

RESULTS

Rapid Induction of EAT in NCR-G3 Cells with Exposure to RA

The time kinetics of EAT protein level during NCR-G3 differentiation was determined by immunoblot analysis using EAT polyclonal antibody, $\alpha EAT_{31\text{-}229}$ (Fig. 2A). EAT protein levels increased dramatically after RA treatment, peaked at 8 h, and then gradually decreased undergoing differentiation. Interestingly, the polyclonal antibody also detected an approximately 35-kDa band which is expected as the EAT splicing variant [21, 22]. The 35-kDa band was blocked by preincubation with the GST–EAT fusion protein against the polyclonal antibody, but not by prereaction with GST protein alone (Fig. 2B), indicating that the antibody reacts specifically with 35-kDa protein. However, we have not obtained supportive consensus that the 35-kDa protein corresponds to the EAT splicing variant.

To determine the presence of the EAT splicing variant in NCR-G3 cells, we also performed RT-PCR with

FIG. 4. Intracellular localization of EAT in NCR-G3 cells. (A) NCR-G3 cells were subjected to differential centrifugation and an aliquot of each fraction was assayed for the presence of both EAT and cytochrome *c* oxidase (COX), a mitochondrial membrane protein, using 3A2 and A-6431 monoclonal antibodies, respectively. The fractions are indicated as follows: N, nuclei; Mt, mitochondria; C, cytosol; Mc, microsome. (B) Intact mitochondria purified from RA-exposed NCR-G3 cells were recovered by centrifugation and analyzed by SDS–PAGE after extraction in 0.1 M Na_2CO_3, pH 11.5 (lane 2). The intact mitochondria were also incubated in the presence (lane 3) or absence (lanes 1 and 2) of trypsin (0.2 mg/ml). (C) RA-exposed NCR-G3 cells were subjected to preembedding immunoelectron microscopic analysis with 3A2 antibody (left) and without the antibody (right). The signals were mainly detected on the outer mitochondrial membrane, but not nuclear membrane. (D) Postembedding immunoelectron microscopic analysis with 3A2 antibody was also carried out in the RA-exposed NCR-G3 cells. The gold particles with 3A2 antibody were localized on the outer mitochondrial membrane (arrows).

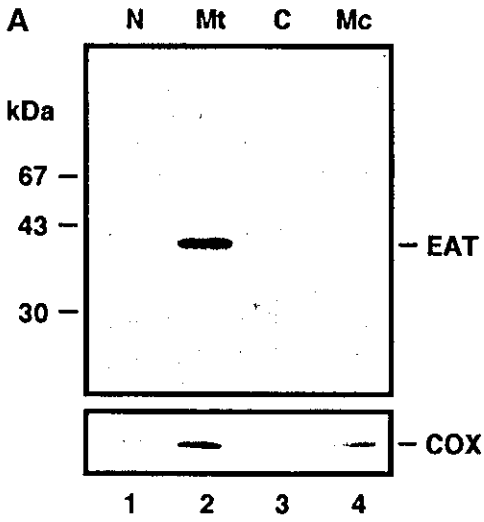
A
N
Mt
C
Mc
kDa
67
43
30
EAT
COX
1
2
3
4

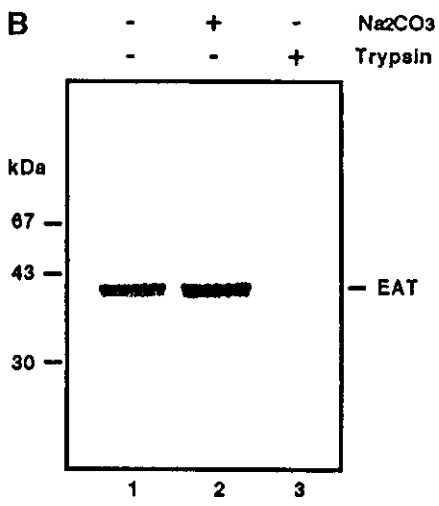
B
-
+
-
Na2CO3
-
-
+
Trypsin
kDa
67
43
30
EAT
1
2
3

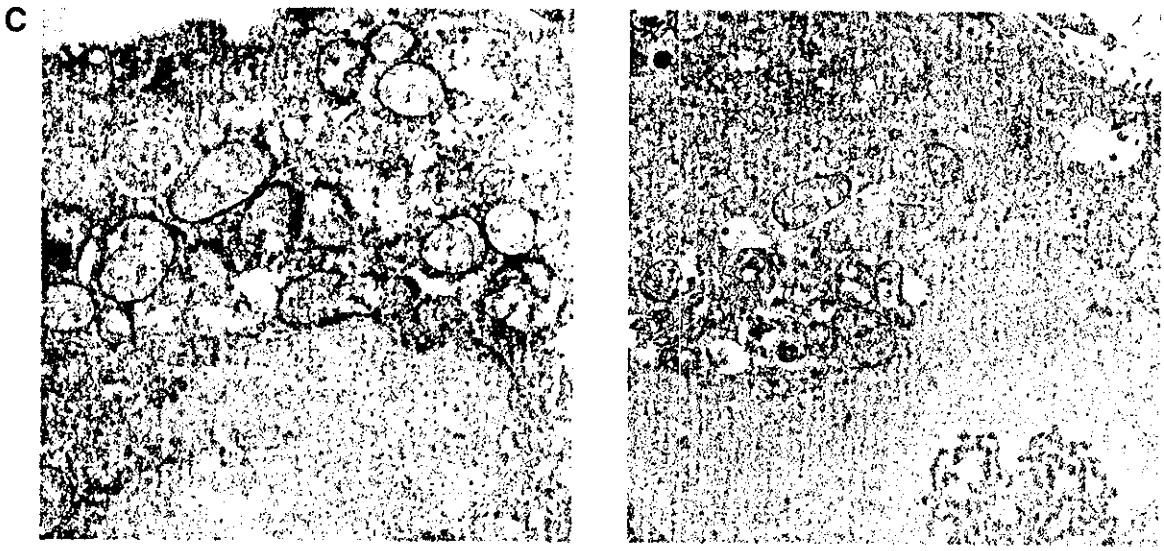
C

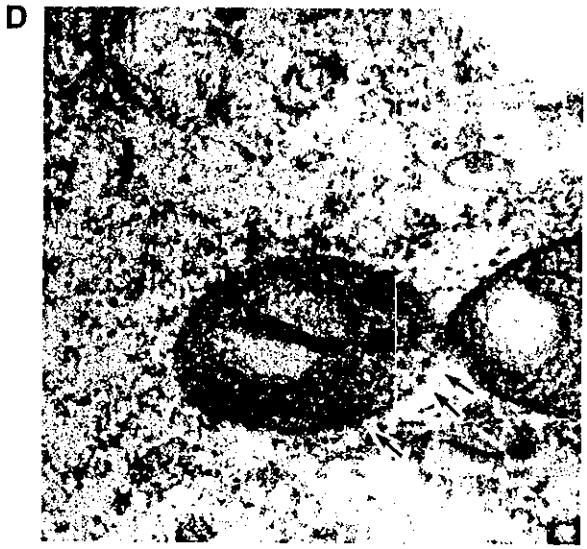
D

EAT-specific primers which amplifies both full-length EAT and the EAT splicing variant (Fig. 2C). The transcripts of a full-length EAT (1155 bp) in the NCR-G3 cells increased at 8 h after exposure to RA and declined gradually undergoing differentiation. The predicted EAT splicing variant (907 bp) also increased weakly at 8 h and 1 day after RA treatment and diminished at 2 days. The sequencing analysis of the 907-bp PCR product revealed that the cDNA matched the mcl-1s/ΔTM (mcl-1s) from GenBank database (Accession No. AF198614).

Expression of bcl-2 Family Members in NCR-G3 Differentiation

Expression levels of nine bcl-2 family members in the RA-exposed NCR-G3 cells were determined by RNase protection assay (Fig. 3A). Among the antiapoptotic molecules, bcl-xL and EAT were expressed at a higher level in the RA-exposed NCR-G3 cells. Meanwhile, bcl-w was detected at a low level and bfl-1 and bcl-2 were below detectable levels. Among proapoptotic molecules, bax was the most abundant molecule, while bad and bik were not detected. We also performed immunoblot analysis to determine protein levels of these molecules in addition to mRNA levels (Fig. 3B). Bcl-xL was slightly induced after exposure to RA, peaked at 1–2 days after exposure to RA, and then gradually decreased. However, Bcl-2 and Bcl-xS were not detected throughout the analyzed period. In contrast, strong Bax immunoreactivity remained constant throughout differentiation. Furthermore, gene expression analysis with the human cDNA array was performed (data not shown). The relative expression levels of bcl-2-related genes were consistent with the results of RNase protection assay and immunoblot analysis.

Intracellular Distribution of EAT in NCR-G3 Cells

To predict the intracellular distribution of EAT in EC cells, subfractionation was performed by differential centrifugation and the presence for EAT in the RA-exposed NCR-G3 cells was assayed by immunoblot analysis using 3A2 monoclonal antibody (Fig. 4A). EAT was predominantly present in the mitochondrial fraction which contained a cytochrome *c* oxidase (complex IV) mitochondrial marker. But EAT was not detected in other fractions. During differentiation of NCR-G3, a significant difference in the distribution of EAT was not observed. To determine the precise localization of mitochondrial EAT, intact mitochondria were purified from RA-exposed NCR-G3 cells and treated with alkali solution or protease (Fig. 4B). The mitochondrial EAT was resistant to alkali extraction, which is indicative of a protein that is integrated into the membrane lipid bilayer [28]. EAT was accessible to exogenous trypsin, which would be expected for proteins retaining the N_{cyto}-C_{in} orientation [29]. We further performed immunoelectron microscopic analysis using the 3A2 antibody. In preembedded immunoelectron microscopy, the EAT signals were mainly distributed on the outer mitochondrial membrane in the RA-exposed NCR-G3 cells, but not to the perinuclear membrane (Fig. 4C, left). In the control samples from which the first antibodies had been removed, positive signals were not detected (Fig. 4C, right). In postembedded immunoelectron microscopic analysis, gold particles with 3A2 antibody were mainly localized to the outer mitochondrial membrane (Fig. 4D). Thus, these results indicate that EAT predominantly targets to outer mitochondrial membrane and that the protein is anchored by the predicted transmembrane segment.

Induction of Apoptosis in NCR-G3 Cells during Differentiation

To investigate the induction of apoptotic cells quantitatively, TUNEL method and sequential flow cytometric analysis were performed. After incubation with RA for 24 h, TRITC-labeled NCR-G3 cells were observed using a fluorescence microscopy to confirm specificity of TUNEL method (Fig. 5A). Condensed chromatin was highly detected in the nuclei of TUNEL-positive apoptotic cells, showing that TRITC labeling with TUNEL method was specific. In flow cytometric analysis, apoptosis was highly induced at 48 h concurrent with previously observed reductions in EAT expression (Fig. 5B). To investigate the relationships between induction of apoptosis and EAT expression during differentiation, we performed immunocytochemistry with anti-EAT antibody and TUNEL

FIG. 5. Inverse correlation between induction of apoptosis and EAT expression in NCR-G3 differentiation. (A) NCR-G3 cells were incubated with 5×10^{-5} M RA and the presence of apoptosis was detected by TRITC-labeled TUNEL method. On a fluorescence microscopy, chromatin condensation and apoptotic bodies were highly detected in the NCR-G3 cells at 24 h after treatment with RA. (B) In flow cytometric analysis, the number of apoptotic cells increased remarkably at 48 h. (C) Frozen section (6 μm) showed the presence of an apoptotic cell in the NCR-G3 cells at 8 h after addition of RA. EAT immunoreactivity with 3A2 antibody was detected with DAB in the nearly all viable cells (top column, a), but not the apoptotic cell (arrow). After removal of nuclear staining, the same section was stained by TUNEL method (b); therefore DNA fragmentation of the apoptotic cells appears as red signals with 3-amino-9-ethylcarbazole (arrow) in addition to the brown signals of EAT immunoreactivity. Schematic diagram is shown, based on the results of double staining with immunocytochemistry and TUNEL (bottom column). (Left) EAT immunoreactivity was detected in the cytoplasm of NCR-G3 cells, but not in a cell with fragmented nucleus. (Right) TUNEL reactivity was observed in the cell with a fragmented nucleus.

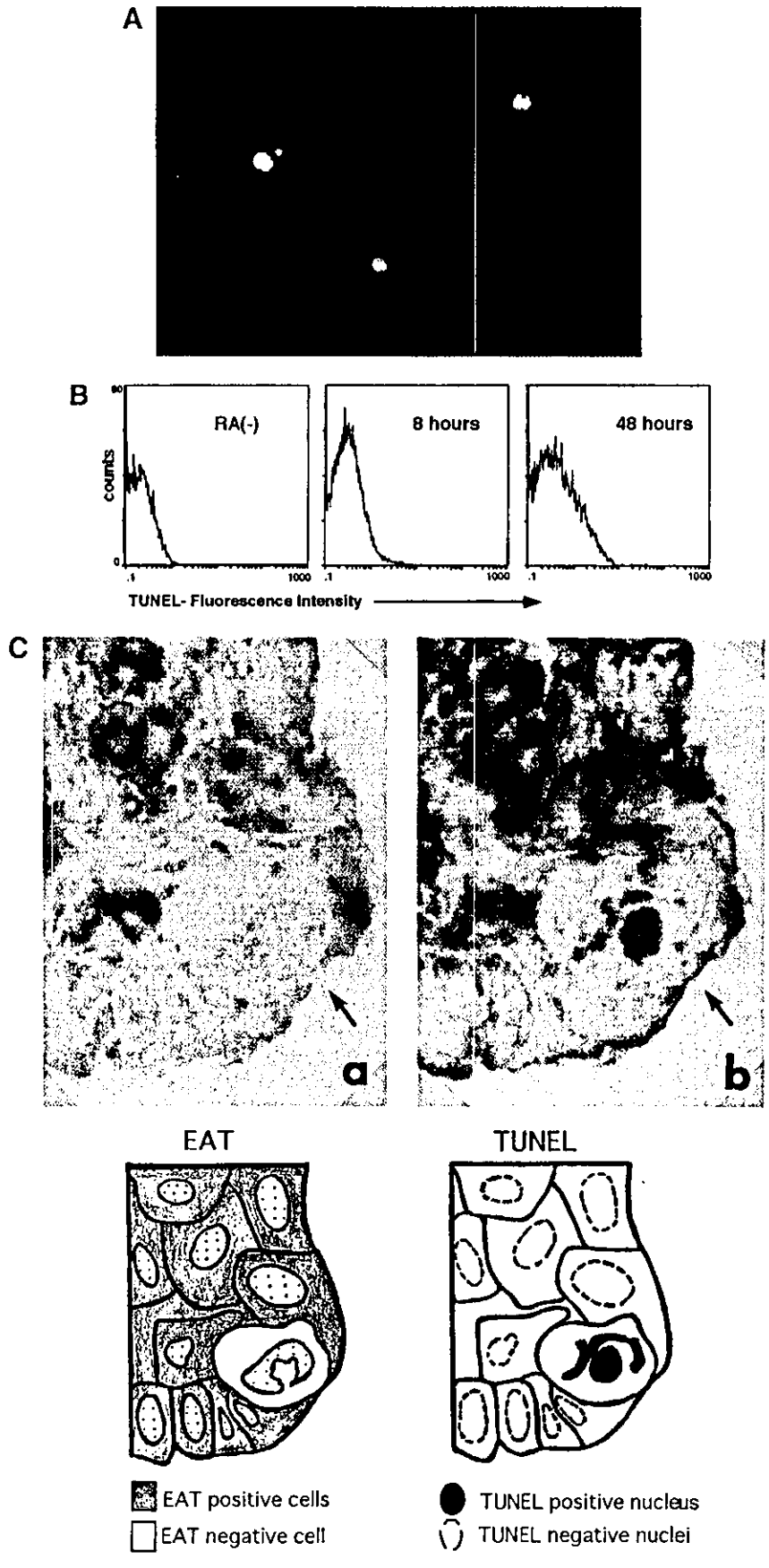
A
B
RA(-)
8 hours
48 hours
counts
TUNEL- Fluorescence Intensity
C
a
b
EAT
TUNEL
EAT positive cells
EAT negative cell
TUNEL positive nucleus
TUNEL negative nuclei

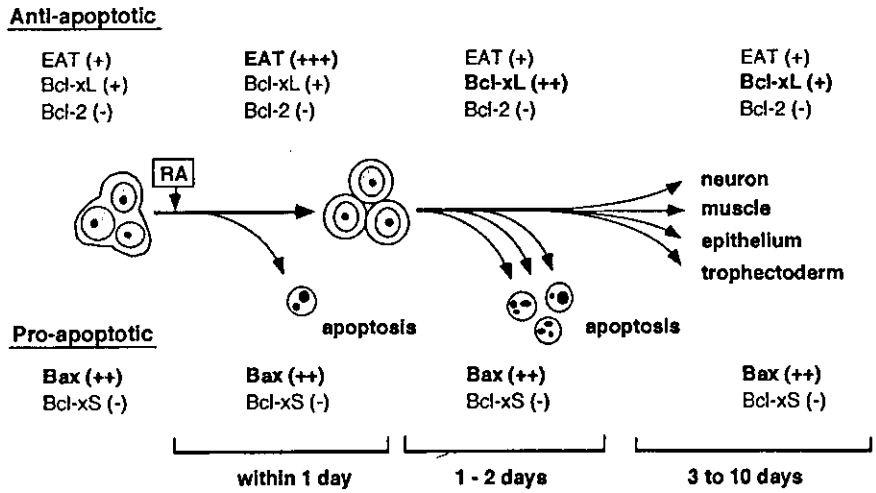

FIG. 6. Schematic representation of "apoptosis" regulation during EC differentiation induced by RA. NCR-G3 exhibits differentiation into multiple lineages upon exposure to RA. Differentiation marker proteins such as keratins, human chorionic gonadotropin, neurofilaments, and desmin are expressed at the late stage of differentiation (3 to 10 days after exposure to RA). EAT was expressed rapidly at the early stage (within 1 day) and decreased at a later stage. In contrast, Bcl-xL was induced at the middle stage (1 to 2 days), reaching the maximum level at the time of down-regulated EAT expression. Bcl-2 was not expressed during differentiation. In contrast, proapoptotic Bax was strongly expressed throughout the analyzed period, while Bcl-xS was not detected throughout all stages of differentiation. Thus, expression levels of bcl-2-related genes may regulate a viability of the EC cells undergoing either apoptosis or subsequent stage of differentiation.

method on the same specimens. First, we carried out immunocytochemistry on NCR-G3 cells using 3A2 antibody. EAT immunoreactivity was detected in nearly all NCR-G3 cells concurrent with maximal EAT synthesis, but little immunoreactivity to EAT was observed in NCR-G3 cells which formed colonies (Fig. 5C, left column). The EAT-negative cells showed narrow and condensed nuclear chromatin, which are characteristic of apoptotic nuclei. After removal of the methyl green staining, the same section was labeled for nicked DNA ends; thus, DNA fragmentation appeared as red signals with 3-amino-9-ethylcarbazole in addition to the positive (brown) reaction of immunocytochemistry (Fig. 5C, right column). Cells with little immunoreactivity to EAT were found to be apoptotic. On the contrary, the TUNEL-negative cells showed strong EAT immunoreactivity. These results suggest that there is an inverse correlation between EAT expression and onset of apoptosis.

DISCUSSION

EC Cell Differentiation, Early Embryogenesis, and Apoptosis

Early embryogenesis in the postfertilized ovum can be studied in the model system of EC cell lines [1–3]. To categorize these early events, the process of NCR-G3 cell differentiation was separated into an hypothetical four stages (Fig. 6). Before addition of an inducer (an undifferentiated stage), NCR-G3 does not show any differentiated phenotypes. After exposure to RA, immediate early genes are induced rapidly within 1 day after treatment of RA, which we define as an early stage of differentiation. Differentiation marker proteins such as neurofilaments, desmin, keratins, and human chorionic gonadotropin begin to be induced from 3 to 10 days after RA treatment [4, 5], which we define as a late stage. A middle stage of differentiation (1 to 3 days after treatment of RA) fills in the process between the early and late stage of differentiation.

Apoptosis, occurring concurrent to differentiation, has been shown to be induced by RA in a variety of EC cell lines such as F9 and P19 [30, 31]. The presence of apoptotic cells has also been noted during the process of NCR-G3 differentiation [6]. Exposure of NCR-G3 to RA initially induces a gradual increase in the number of apoptotic cells; however, a more remarkable increase in apoptotic cells is noted at the middle stage of differentiation which correlates with a down-regulation in EAT. Clinically, in human development, excessive apoptosis has been detected in early embryos that fail to execute essential developmental events. The regulation of both cell differentiation and apoptosis is thus believed to be critical in early embryogenesis.

Bcl-2-related genes display either positive or negative regulatory effects on apoptosis *in vitro* and *in vivo* [32–35]. The expression of these genes has been analyzed during murine embryogenesis [36]. The Bcl-xL gene is highly transcribed after fertilization, peaks at the late-one-cell stage and then declines rapidly in

expression. In contrast, only a small amount of bcl-2 mRNA is present until the mid-one-cell stage and, likewise, decreases at a later stage. EAT is induced rapidly after fertilization, peaks at the two-cell stage, is maintained until the eight-cell stage, and then decreases to less than unfertilized egg levels in blastocyst [24]. EAT has also shown to be essential for preimplantation development [37]. Bax, a proapoptotic molecule, has been shown to be functionally involved in the apoptotic event of preimplantation embryos [38]. The induction of the various bcl-2-related proteins may be a pivotal event in murine embryogenesis, especially from fertilization to the eight-cell stage. It is noteworthy that the expression profile and time course of bcl-2-related genes in this period are consistent with that observed with NCR-G3 which mimic the events in early embryogenesis.

Functions of Antiapoptotic bcl-2-Related Genes in the Sequential Stages of EC Cell Differentiation

Previous studies have established that Bcl-2, Bcl-xL, Bcl-w, and Bfl-1 are antiapoptotic molecules while Bax, Bak, Bid, Bik, and Hrk are proapoptotic molecules [35, 39–49]. EAT, a bcl-2-related molecule, has antiapoptotic function [15–18], while the EAT splicing variant promotes apoptosis [21, 22]. The expression of EAT was dramatically induced at the early stage of NCR-G3 differentiation. Expression of approximately 35-kDa protein, which is an expected molecular size as the EAT splicing variant, was also induced at 8 h and remained until 2 days. RT-PCR followed by sequencing analysis revealed that there is a presence of the EAT splicing variant in the EC cell, but the expression level was very low, compared with full-length EAT. Proapoptotic functions of the EAT splicing variant is inhibited by dimerization with full-length EAT only among the known antiapoptotic molecules [21]. The number of apoptotic cells increased at the middle stage of differentiation that concurrent with a reduction in EAT and a strong induction of the 35-kDa protein. Based on the evidence that the action of the down-regulation of EAT induces apoptosis in hematopoietic cells [50], we suggest that the down-regulation of EAT may also trigger apoptosis in the NCR-G3 cells undergoing differentiation. In addition to alternative splicing, EAT can be modified by phosphorylation [51], proteolytic cleavage, or relocalization like bcl-2. The potential role of these factors in EC cell differentiation remains to be investigated.

Bcl-2 family members localized to the mitochondria are believed to initiate apoptosis. Bcl-2 and Bcl-xL are predominantly localized to the outer mitochondrial membrane [11, 12]. In cell-free systems, only bcl-2 localized to the mitochondrial membrane is able to inhibit the induction of apoptosis, while bcl-2 localized to the nuclear membrane is not able to inhibit similar apoptotic induction [10]. Though Bax is found diffusely throughout the cytosol and organelles, it shifts from cytosol to mitochondria upon induction of apoptosis [52]. Therefore, it is surmised that bcl-2-related proteins that localize to the outer mitochondrial membrane are most significant in the initiation of apoptosis. Antiapoptotic EAT was localized to the outer mitochondrial membrane in human EC cells. The localization of EAT is consistent with the results of previous reports that EAT colocalizes with mitochondrial proteins [53, 54]. EAT as well as Bcl-2 and Bcl-xL has been reported to heterodimerize with Bax [55, 56] and inhibit proapoptotic functions on the outer mitochondrial membrane [57]. It may be reasonable to assume that induction of EAT prevents apoptosis in EC cells undergoing differentiation by neutralizing proapoptotic Bax, while the high expression of Bax remains unchanged as a default expression level throughout EC cell differentiation.

EAT is also known to be an immediate early gene. A role for EAT expression is further reinforced by the fact that EAT has an immediate response box in its 3′-untranslated region similar to other immediate early genes such as c-*fos*, c-*jun*, and colony-stimulation factor-1 [20]. Likewise, it also possesses PEST sequences which are signatory of proteins which undergo rapid degradation [19, 50]. In our findings, EAT was induced rapidly in NCR-G3 cells after treatment with RA and then diminished. The transient expression of EAT is also reported in the differentiation of EC cells, ES cells, and hematopoietic cells as well as in acute myocardial infarction [20, 50, 54, 58, 59]. Interestingly, EAT has been shown to be induced rapidly after fertilization [24]. In EC cells, Bcl-xL was slightly induced at the middle stage of differentiation (1 to 2 days after exposure to RA), whereas bcl-2 protein was not detected throughout differentiation. Thus, we propose that the rapid induction of EAT and the supplemental expression of Bcl-xL are the pivotal antiapoptotic molecules and events in preventing EC cells from undergoing RA-induced apoptosis. Thus, the expression of these antiapoptotic molecules may maintain the viability of the cells during the differentiation of EC cells.

The authors thank A. Suzuki for critical reviewing of the manuscript, J. Ozawa for excellent technical assistance with RNase protection assay, Y. Kanzaki for assistance with immunoelectron microscopy, H. Suzuki and S. Kusakari for advise with immunocytochemistry and cell culture, K. Takeichi for the photographs, and H. Simada, K. Segawa, T. Yamada, S-i. Imai, N. Hiraoka, T. Ando, Y. Hiraoka, M. Ogawa, F. Urano, and Y. Nakata for their technical advise and discussion. This work was supported by a grant from the Ministry of Education, Science and Culture to J. H. and A. U., by Keio University Special Grant-in-Aid for Innovative Collaborative Research Project to J. H. and A. U., by Research Fellowships of the Japan Society for the Promotion of Science for Young Scientist to M. S., and by a National Grant-in-Aid for the

Establishment of a High-Tech Research Center at Private Universities. Expression profile of NCR-G3 is available as a database at http://www.med.keio.ac.jp/patho/au/G3profile.html (ID, ecr; password, ecr).

REFERENCES

1. Martin, G. R. (1980). Teratocarcinomas and mammalian embryogenesis. *Science* **209**(4458), 768–776.
2. Martin, G. R. (1975). Teratocarcinomas as a model system for the study of embryogenesis and neoplasia. *Cell* **5**(3), 229–243.
3. Mintz, B., and Illmensee, K. (1975). Normal genetically mosaic mice produced from malignant teratocarcinoma cells. *Proc. Natl. Acad. Sci. USA* **72**(9), 3585–3589.
4. Maruyama, T., Umezawa, A., Kusakari, S., Kikuchi, H., Nozaki, M., and Hata, J. (1996). Heat shock induces differentiation of human embryonal carcinoma cells into trophectoderm lineages. *Exp. Cell Res.* **224**(1), 123–127.
5. Hata, J., Fujimoto, J., Ishii, E., Umezawa, A., Kokai, Y., Matsubayashi, Y., Abe, H., Kusakari, S., Kikuchi, H., Yamada, T., and Maruyama, T. (1992). Differentiation of human germ cell tumor cells in vivo and in vitro. *Acta Histochem. Cytochem.* **25**(5), 563–576.
6. Yamada, T., Suzuki, N., Hiraoka, N., Matsuoka, K., Fukushima, S., Hashiguchi, A., and Hata, J.-I. (1996). Apoptosis of human embryonal carcinoma cells with in vitro differentiation. *Cell Struct. Funct.* **21**, 53–61.
7. Zamzami, N., Susin, S. A., Marchetti, P., Hirsch, T., G-Monterrey, I., Casted, M., and Kroemer, G. (1996). Mitochondrial control of nuclear apoptosis. *J. Exp. Med.* **183**, 1533–1544.
8. Heiden, M. G. V., Chandel, N. S., Williamson, E. K., Schumacker, N. S., and Thompson, C. B. (1997). Bcl-xL regulates the membrane potential and volume homeostasis of mitochondria. *Cell* **91**, 627–637.
9. Liu, X., Kim, C. N., Yang, J., Jemmerson, R., and Wang, X. (1996). Induction of apoptotic program in cell-free extracts: Requirement for dATP and cytochrome *c*. *Cell* **86**, 147–157.
10. Susin, S. A., Zamzami, N., Castedo, M., Hirsch, T., Marchetti, P., Macho, A., Daugas, E., Geuskens, M., and Kroemer, G. (1996). Bcl-2 inhibits the mitochondrial release of an apoptogenic protease. *J. Exp. Med.* **184**(4), 1331–1341.
11. Gonzalez-Garcia, M., Perez-Ballestero, R., Ding, L., Duan, L., Boise, L. H., Thompson, C. B., and Nunez, G. (1994). bcl-XL is the major bcl-x mRNA form expressed during murine development and its product localizes to mitochondria. *Development* **120**(10), 3033–3042.
12. Monaghan, P., Robertson, D., Amos, T. A., Dyer, M. J., Mason, D. Y., and Greaves, M. F. (1992). Ultrastructural localization of bcl-2 protein. *J. Histochem. Cytochem.* **40**(12), 1819–1825.
13. Shimizu, S., Narita, M., and Tsujimoto, Y. (1999). Bcl-2 family proteins regulate the release of apoptogenic cytochrome c by the mitochondrial channel VDAC. *Nature* **399**(6735), 483–487.
14. Umezawa, A., Maruyama, T., Inazawa, J., Imai, S., Takano, T., and Hata, J. (1996). Induction of mcl1/EAT, Bcl-2 related gene, by retinoic acid or heat shock in the human embryonal carcinoma cells, NCR-G3. *Cell Struct. Funct.* **21**(2), 143–150.
15. Ando, T., Umezawa, A., Suzuki, A., Okita, H., Sano, M., Hiraoka, Y., Aiso, S., Saruta, T., and Hata, J.-i. (1998). EAT/mcl-1, a member of the bcl-2 related genes, confers resistance to apoptosis induced by cis-diammine dichloroplatinum (II) via a p53-independent pathway. *Jpn. J. Cancer Res.* **89**, 1326–1333.
16. Zhou, P., Qian, L., Kozopas, K. M., and Craig, R. W. (1997). Mcl-1, a Bcl-2 family member, delays the death of hematopoietic cells under a variety of apoptosis-inducing conditions. *Blood* **89**, 630–642.
17. Reynolds, J. E., Li, J., Craig, R. W., and Eastman, A. (1996). Bcl-2 and Mcl-1 expression in Chinese hamster ovary cells inhibits intracellular acidification and apoptosis induced by staurosporine. *Exp. Cell Res.* **225**, 430–436.
18. Reynolds, J. E., Yang, T., Qian, L., Jenkinson, J. D., Zhou, P., Eastman, A., and Craig, R. W. (1994). Mcl-1, a member of the Bcl-2 family, delays apoptosis induced by c-Myc overexpression in Chinese hamster ovary cells. *Cancer Res.* **54**(24), 6348–6352.
19. Kozopas, K. M., Yang, T., Buchan, H. L., Zhou, P., and Craig, R. W. (1993). MCL1, a gene expressed in programmed myeloid cell differentiation, has sequence similarity to BCL2. *Proc. Natl. Acad. Sci. USA* **90**, 3516–3520.
20. Okita, H., Umezawa, A., Suzuki, A., and Hata, J. (1998). Upregulated expression of murine Mcl1/EAT, a bcl-2 related gene, in the early stage of differentiation of murine embryonal carcinoma cells and embryonic stem cells. *Biochim. Biophys. Acta* **1398**(3), 335–341.
21. Bae, J., Leo, C., Hsu, S., and Hsueh, A. (2000). Mcl-1S, a splicing variant of the antiapoptotic Bcl-2 family member Mcl-1, encodes a proapoptotic protein possessing only the BH3-domain. *J. Biol. Chem.* **275**, 25255–25261.
22. Bingle, C. D., Craig, R. W., Swales, B. M., Singleton, V., Zhou, P., and Whyte, M. K. (2000). Exon skipping in mcl-1 results in a bcl-2 homology domain 3 (BH3)-only gene product that promotes cell death. *J. Biol. Chem.* **275**, 22136–22146.
23. Suzuki, A., Umezawa, A., Sano, M., Nozawa, S., and Hata, J. (2000). Involvement of EAT/mcl-1, a bcl-2 related gene, in the apoptotic mechanisms underlying human placental development and maintenance. *Placenta* **21**, 177–183.
24. Sano, M., Umezawa, A., Suzuki, A., Shimoda, K., Fukuma, M., and Hata, J.-i. (2000). Involvement of EAT/mcl-1, an antiapoptotic bcl-2 related gene, in murine embryogenesis and human development. *Exp. Cell Res.* **259**, 127–139.
25. McBride, H. M., Millar, D. G., Li, J.-M., and Shore, G. C. (1992). A signal-anchor sequence selective for the mitochondrial outer membrane. *J. Cell Biol.* **119**, 1451–1457.
26. Shimizu, H., McDonald, J. N., Kennedy, A. R., and Eady, R. A. (1989). Demonstration of intra- and extracellular localization of bullous pemphigoid antigen using cryofixation and freeze substitution for postembedding immunoelectron microscopy. *Arch. Dermatol. Res.* **281**(7):443–448.
27. Shimizu, H., Ishida-Yamamoto, A., and Eady, R. A. (1992). The use of silver-enhanced 1-nm gold probes for light and electron microscopic localization of intra- and extracellular antigens in skin. *J. Histochem. Cytochem.* **40**, 883–888.
28. Li, J.-M., and Shore, G. C. (1992). Reversal of the orientation of an integral protein of the mitochondrial outer membrane. *Science* **256**, 1815–1817.
29. Nguyen, M., Millar, D. G., Yong, V. W., Korsmeyer, S. J., and Shore, G. C. (1993). Targeting of Bcl-2 to the mitochondrial outer membrane by a COOH-terminal signal anchor sequence. *J. Biol. Chem.* **268**, 25265–25268.
30. Okazawa, H., Shimizu, J., Kamei, M., Imafuku, I., Hamada, H., and Kanazawa, I. (1996). Bcl-2 inhibits retinoic acid-induced apoptosis during the neural differentiation of embryonal stem cells. *J. Cell Biol.* **132**(5), 955–968.
31. Atencia, R., Garcia-Sanz, M., Unda, F., and Arechaga, J. (1994). Apoptosis during retinoic acid-induced differentiation of F9 embryonal carcinoma cells. **214**(2), 663–667.
32. Adams, J. M., and Cory, S. (1998). The Bcl-2 protein family: Arbiters of cell survival. *Science* **281**(5381), 1322–1326.

Pediatric and Developmental Pathology 4, 381–390, 2001
DOI: 10.1007/s10024-001-0003-8

Pediatric and Developmental Pathology

CASE REPORTS

Nesidioblastosis and Mixed Hamartoma of the Liver in Beckwith-Wiedemann Syndrome: Case Study Including Analysis of H19 Methylation and Insulin-like Growth Factor 2 Genotyping and Imprinting

RYUJI FUKUZAWA,[1] AKIHIRO UMEZAWA,[1] YUKIHIKO MORIKAWA,[2] KYONG CHANG KIM,[3] TOSHIRO NAGAI,[4] AND JUN-ICHI HATA[1]*

[1]Department of Pathology, Keio University School of Medicine, 35 Shinanomachi, Shinjuku-ku, Tokyo 160-8582, Japan
[2]Department of Pathology, Tokyo Metropolitan Kiyose Children's Hospital, 1-3-1 Umezono, Kiyose-shi, Tokyo 204-0024, Japan
[3]Department of Neonatology, Tokyo Metropolitan Kiyose Children's Hospital, 1-3-1 Umezono, Kiyose-shi, Tokyo 204-0024, Japan
[4]Department of Pediatrics, Koshigaya Hospital, Dokkyo University School of Medicine, 2-1-50 Minamikoshigaya, Koshigaya-shi, Saitama 343-0845, Japan

Received February 25, 2000; accepted October 19, 2000.

ABSTRACT

An infant with persistent hyperinsulinemic hypoglycemia, diffuse nesidioblastosis, and mixed hamartoma of the liver (MHL), in addition to demonstrating clinical, pathologic, and molecular manifestations of Beckwith-Wiedemann syndrome (BWS), is the subject of this report. *H19* methylation assay and allelic expression analysis for insulin-like growth factor 2 (*IGF2*) indicated that the patient was mosaic for paternal isodisomic cells and normal cells in lung tissue, nontumoral liver tissue, tissue from the MHL, and pancreatic tissue. We propose that abundant *IGF2* expression during development due to paternal isodisomy resulted in hepatomegaly and islet cell hyperplasia, which led to nesidioblastosis. MHL, by contrast, may have resulted from a decrease in disomic cells, compared with nontumoral liver tissue, which showed an increase in disomic cells. Thus, somatic mosaicism may result in unbalanced tissue growth, which may contribute to the formation of MHL in BWS.

Key words: Beckwith-Wiedemann syndrome, mixed hamartoma of the liver, nesidioblastosis, uniparental disomy, H19, insulin-like growth factor 2

INTRODUCTION

Beckwith-Wiedemann Syndrome (BWS) is a congenital overgrowth syndrome characterized by omphalocele, macroglossia, visceromegaly, cytomegaly of the adrenal cortex, and Leydig cell hy-

*Corresponding author

perplasia. A number of other abnormalities have been reported including hemihypertrophy, nephroblastomatosis and/or medullary dysplasia of the kidneys, nesidioblastosis, and nevus flameus (capillary hemangiomatosis); BWS is also associated with a number of embryonal tumors. These abnormalities occur in various combinations, resulting in complete and incomplete forms of the syndrome [1]. BWS is a chromosomal disorder involving uniparental paternal disomy (UPD) of 11p15.5, duplication of paternally derived 11p15.5, or translocation of maternal chromosome 11 with a breakpoint in 11p15.5 [2]. Current developments in cytogenetic, clinical, genetic, and molecular studies, and in particular, an increased understanding of UPD, have clarified the role of somatic mosaicism in partial (especially in association with hemihypertrophy) and complete expression of BWS [3–8]. To date, most BWS patients with UPD have had mosaic and segmental paternal uniparental isodisomy as a result of postzygotic mitotic recombination [6]. Hyperinsulinemic hypoglycemia is another major clinical problem in many newborns affected by BWS [2], however, the hypoglycemia is transient and is usually referred to as islet cell hyperplasia [9].

Mixed hamartoma of the liver (MHL) is a very rare condition that was differentiated from focal nodular hyperplasia by Rhodes et al. [10]. In general, MHL is congenital in origin and is considered to be hamartomatous rather than a true tumor. Little is known about the molecular pathology of hamartomas in BWS, but somatic mosaicism may also explain some hamartomatous conditions in BWS. In this report, we describe the autopsy and histopathologic findings of an infant with MHL and nesidioblastosis, and discuss the molecular basis for dysorganogenesis in BWS.

CASE REPORT

The patient was a female Japanese infant delivered by cesarean section at 34 weeks of gestation. The mother was 24 years old, and the father was 26 years old. The birth weight was 2772 g (+1.5 SD), and the crown–heel length at birth was 48 cm (+1.5 SD). The mother's glucose tolerance test was normal during pregnancy. Her family history was noncontributory. Ultrasound examination performed at 33 weeks documented a hepatic mass and placental overgrowth. At birth, the patient presented with intractable hyperinsulinemic hypoglycemia (insulin, 124 IU/ml; glucose, 0 mg/dl), and subtotal pancreatectomy was performed at 1 month of age. The resected pancreas showed the features of nesidioblastosis. Stable blood glucose levels were maintained postoperatively, but the patient's condition gradually deteriorated because she was exposed to repeated hypoglycemic attack and had brain damage. Finally, she developed aspiration pneumonia and died of sepsis at 13 months of age. The patient's karyotype was normal (46, XX). The indications of BWS included a small umbilical hernia and unilateral ear lobe crease; no macroglossia or hemihypertrophy was present.

PATHOLOGIC FINDINGS

All tissues obtained at autopsy and the surgically resected pancreas were fixed with 10% formalin and embedded in paraffin. All blocks were cut into 3-μm-thick sections and stained with hematoxylin-eosin. Immunohistochemical studies were performed using avidin-biotin peroxidase complex techniques with formalin-fixed, paraffin-embedded sections. Thinly sliced sections of surgically resected pancreatic head, body, and tail, and specimens of the pancreatic head obtained at autopsy were immunostained for insulin, glucagon, somatostatin, and pancreatic polypeptide. Primary antibodies against glucagon (polyclonal; DAKO), somatostatin (polyclonal; DAKO), and pancreatic polypeptide (polyclonal; DAKO) were used.

Autopsy findings

Postmortem examination revealed generalized visceromegaly, including cardiomegaly (63 g), hepatomegaly with multiple tumors (450 g), splenomegaly (60 g), and nephromegaly with exaggerated lobulation (68 g and 74 g). Microscopic findings showed adrenal cytomegaly, hilus cell hyperplasia of the ovaries, and nesidioblastosis. There were no persistent nephrogenic rests or medullary dysplasia in the kidneys. These clinical and autopsy findings were consistent with an incomplete form of BWS.

Pancreatic pathology

"Nesidioblastosis" is generally used to describe persistent hyperinsulinemic hypoglycemia of new-

borns with histological characteristics of a ductuloinsular complex. The nesidioblastosis was histologically classified according to Goossens et al. [11].

The histopathological findings at 1 month of age showed diffuse nesidioblastosis. The surgically resected pancreatic tissue showed increased variation in islet size, with prominent ductuloinsular complexes in the lobules throughout the pancreas. Abnormally large islets were concentrated in the center of the lobules and were surrounded by ductular epithelium and acinar tissue at many sites (Fig. 1A). Most of the cells showed immature features with hypertrophic cytoplasm and large nuclei, and occasionally formed islet-like clusters. Immunohistochemical analysis revealed B-cell hypertrophy (Fig. 1C). The proportions of B cells, somatostatin cells, and pancreatic polypeptide cells were increased. There was an obvious increase in the number of B cells, but a relative decrease in the number of A cells (Fig. 1D), although some previous reports have described a tendency toward a decrease in D cells in diffuse nesidioblastosis [9].

The histopathological findings at 11 months were much different. Obvious acinar differentiation and proliferation were observed surrounding the islets (Fig. 1B). They still showed hyperplasia at some sites, but endocrine cells and ductular epithelia also showed differentiation. The nuclei and cytoplasm of the endocrine cells had become smaller than at the age of 1 month. Despite the relative increase in the number of B cells at 13 months, the normal distribution of the four main islet cells was maintained—i.e., there were centrally located insulin cells surrounded by glucagon (Fig. 1E, F), somatostatin, and pancreatic polypeptide cells (data not shown).

Liver pathology

Multiple hepatic masses were noted in an enlarged liver. One mass was attached to the right lobe (3.2 cm in diameter), and the others were located in the left lobe (Fig. 2A), the floor of the gallbladder, and the porta hepatis (2.5 cm, 2.5 cm, and 2.0 cm in diameter, respectively). The lesions were separated from the surrounding normal liver tissue by a discontinuous fibrous capsule (Fig. 2B). The tumor on the left lobe had a white center separated by a thin fibrous band. Histopathological examination revealed a multinodular lesion with lobulation, and the nodules were composed of relatively small hepatocytes. Numerous metaplastic bile ducts were observed in the transitional areas between the hepatic lobules and the fibrous septa (Fig. 2C). The macroscopic appearance of the tumor on the left lobe showed some characteristics of focal nodular hyperplasia; however, the microscopic findings were characteristic of pseudolobulations with hepatocellular bile-ductular transformation and were consistent with MHL.

METHODS

Tissue samples and nucleic acid purification

Tumor, adjacent nontumor areas of liver tissue, and lung tissue were obtained from the patient at autopsy 11 h after her death. Pancreatic tissue (histologically diagnosed as diffuse nesidioblastosis) was obtained at surgery. Control fetal liver tissue at 21 weeks gestation was obtained after an elective abortion. Age-matched control lung and pancreatic tissue was obtained from a 1-month-old girl who died of respiratory failure. All tissues were quickly frozen in liquid nitrogen and stored at −80°C until analysis was conducted. DNA and RNA were extracted from tumors and normal tissues as previously described [12,13].

Tyrosine hydroxylase (*TH*) heterozygosity

DNA was amplified as follows [7] to analyze the tetranucleotide polymorphism at *TH*. Polymerase chain reaction (PCR) consisted of 30 cycles (94°C, 1 min; 60°C, 1 min; 72°C, 1 min). The primers were (TH-F; 5′-CTGGGCTCTGGGGTGATTCC-3′) and (TH-R; 5′-CCGAGTGCAGGTCACAGGGA-3′). PCR products were electrophoresed on 2% agarose gel.

Insulin-like growth factor 2 (*IGF2*) allelic expression

Complementary DNA was generated with a first-strand cDNA synthesis kit (Pharmacia Biotec, Uppsala, Sweden). An *Apa*I/*Ava*II polymorphism in exon 9 was used to analyze *IGF2* allele-specific expression as previously described [12,13]. To exclude partial digestion of the PCR products, they were digested using an internal control (λDNA) by *Apa*I.

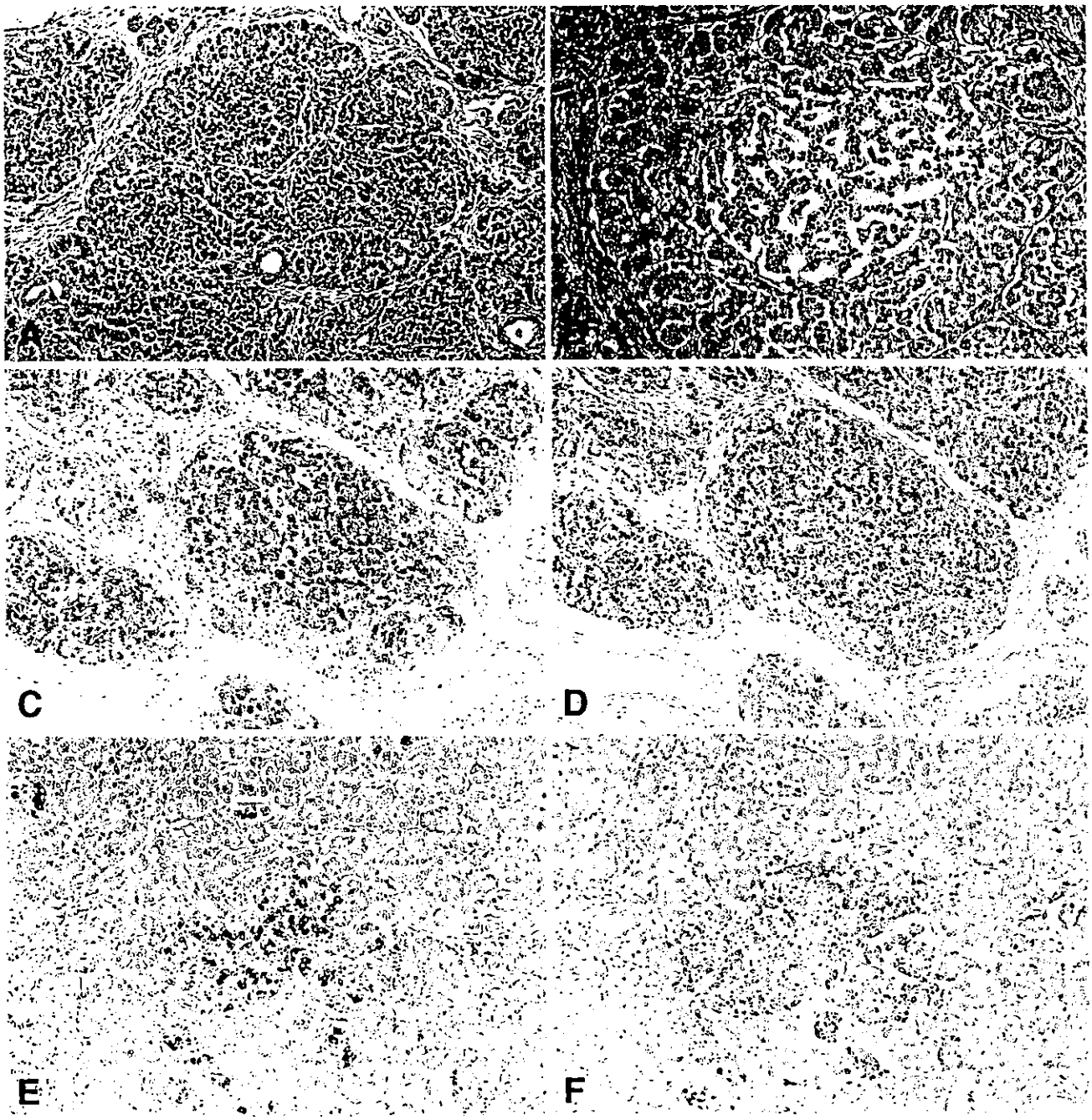

Figure 1. Microscopic evidence of nesidioblastosis at surgery (1 month of age) (**A,C,D**) and at autopsy (13 months of age) (**B,E,F**). At 1 month there is a marked increase in endocrine cells with hypertrophied cytoplasm and enlarged nuclei, forming large islets that occupy most of the central region of the pancreatic lobules. Only a narrow rim of exocrine cells (A) is left. In contrast, at 13 months of age, the acinar tissue on the periphery of islets has increased markedly and differentiated. The islet cells have sometimes formed tubules (B). Immunohistochemical studies of nesidioblastosis in tissue obtained at surgery (C,D) and at autopsy (E,F) indicate a marked increase in insulin cells (C) and a decrease in glucagon cells (D). At 13 months of age, the typical distribution of normal islets has been maintained. Centrally located insulin cells are surrounded by glucagon cells distributed in the islets at the periphery or along capillaries at the border of the intrainsular ribbons and lobules (E,F).

H19 methylation

An *Hpa*II restriction site in the *H19* promoter region, previously shown to be an imprint-specific methylated region, was analyzed by Southern blotting with *Hpa*II digestion (Fig. 3D) [13,14]. Five micrograms of genomic DNA was digested with *Rsa*I, either alone or together with the methylation-sensitive restriction enzyme *Hpa*II or its meth-